ANL-7787

THE EFFECTS OF DRIVER-FUEL CLADDING DEFECTS ON THE OPERATION OF EBR-II

R. R. Smith, R. M. Fryer,
E. R. Ebersole, W. B. Loewenstein,
and R. V. Strain

ARGONNE NATIONAL LABORATORY, ARGONNE, ILLINOIS

Prepared for the U.S. ATOMIC ENERGY COMMISSION
under contract W-31-109-Eng-38

Printed in the United States of America
Available from
National Technical Information Service
U.S. Department of Commerce
5285 Port Royal Road
Springfield, Virginia 22151
Price: Printed Copy $3.00; Microfiche $0.95

ANL-7787
Reactor Technology

ARGONNE NATIONAL LABORATORY
9700 South Cass Avenue
Argonne, Illinois 60439

THE EFFECTS OF DRIVER-FUEL CLADDING DEFECTS ON THE OPERATION OF EBR-II

by

R. R. Smith, R. M. Fryer,
E. R. Ebersole,* W. B. Loewenstein,
and R. V. Strain

EBR-II Project

February 1972

*Argonne West

2

TABLE OF CONTENTS

TABLE OF CONTENTS

TABLE OF CONTENTS

LIST OF FIGURES

LIST OF FIGURES

LIST OF FIGURES

LIST OF TABLES

THE EFFECTS OF DRIVER-FUEL CLADDING DEFECTS ON THE OPERATION OF EBR-II

by

R. R. Smith, R. M. Fryer,
E. R. Ebersole, W. B. Loewenstein,
and R. V. Strain

ABSTRACT

The various modes of fission-product release from an EBR-II driver-fuel element are reviewed in detail. The results of studies concerned with pressure buildup in the plenum of a fuel element are cited, and it is shown that near the end of life, the pressure may become high enough to unbond fuel material by driving bond sodium from the heat-transfer annulus through a low-elevation defect.

The effects of voids in the heat-transfer annulus are discussed in the framework of simulation experiments conducted in TREAT and first-principle heat-transfer calculations. These studies show that the short-term consequences of fuel unbonding are benign.

Mathematical models for the various modes of fission-product release are described and correlated with observations on actual fission-product releases. Guidelines for the number of defective driver-fuel elements that may be tolerated without affecting the annunciative capability or without aggravating radiological conditions are also described.

I. INTRODUCTION

During the past seven years (1964-1971), a great deal of effort has been devoted to evaluating the effects of activity releases to the primary system (ARP's) from driver-fuel elements on the operation of EBR-II. As a result of these efforts, it is now evident that ARP's from driver-fuel elements can be safely tolerated. Recognition of this conclusion is now reflected in the emergency operating procedures, which permit continued operation of the reactor for ARP's that fall within the envelope expected for driver fuel. This report summarizes, as concisely as possible, the results of the many studies on which this rationale is based.

In preparation of this report, particular care has been taken to satisfy the needs of the casual and more interested reader alike. The interests of the casual reader have been served by condensing in one document a great deal of background information and the principal conclusions reached from a wide variety of studies by many investigators. At the same time, the reader who has more than a casual interest will profit from the inclusion of results that hitherto have been reported in internal memoranda only. The more interested reader will also find it convenient to pursue in-depth interests through the up-to-date references at the end of this report.

II. DESIGN DETAILS

A detailed description of the EBR-II plant is given in the Hazard Summary Report[1] and its Addendum.[2] For convenience, however, a description is given below of the features that relate to the mechanisms involved in the release of fission products from driver-fuel elements and the distribution of fission products through the primary coolant and cover-gas systems.

A. Plant Features

The EBR-II core and blanket internals consist of an array of subassemblies, each of which is a hexagonal Type 304 stainless steel tube containing either driver-fuel elements, encapsulated or unencapsulated irradiation specimens, or depleted-uranium blanket elements. The arrangement of core and blanket subassemblies with respect to other principal components is shown in Fig. 1.

The entire system illustrated in Fig. 1 is immersed in a tank containing approximately 86,000 gal of sodium. Two centrifugal pumps, submerged in the sodium, deliver coolant at 700°F to the inlet plenum at a combined rate of approximately 9000 gpm. By means of throttle valves and a stepped lower grid plate, the inlet stream is divided into a high-pressure system, which cools the core region, and a low-pressure system, which cools the radial blanket.

Both systems discharge into a common upper plenum from which the heated coolant, at a temperature of 883°F (at 62.5 MWt), flows to the intermediate heat exchanger (also submerged in the primary sodium). The coolant leaves the heat exchanger at approximately 695°F (at 62.5 MWt) and discharges directly back to the bulk sodium.

Above the upper surface of the sodium and beneath the primary-tank cover is an argon-filled cover-gas plenum approximately 14 in. high and 26 ft in diameter; its volume is approximately 625 ft^3. Under normal operating conditions, the cover gas contains minute quantities of rare-gas fission products that are generated by fission in a small quantity of fuel material that unavoidably contaminates core components.

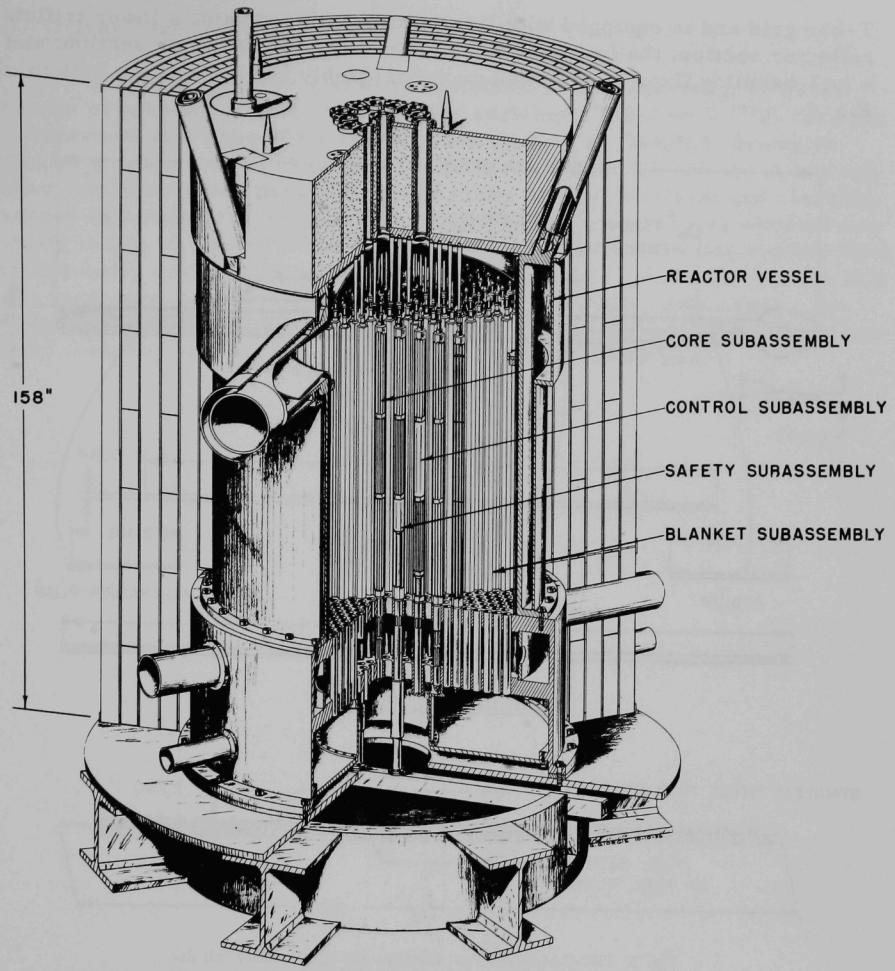

Fig. 1. Cutaway View of EBR-II Reactor Vessel

B. Core Subassembly

The standard driver-fuel subassembly consists essentially of a hexagonal tube filled with a close-packed hexagonal array of 91 standard Mark-IA driver-fuel elements. The hexagonal tube has a wall thickness of 0.040 in. and measured 2.290 in. across the external flats. The subassembly, from the bottom of the pole piece to the top of the fuel-handling fixture, has an overall length of 92 in. Principal features of a complete subassembly include the following: a lower pole piece, which fixes the subassembly on a

T-bar grid and is equipped with flow holes for the coolant; a lower trifluted reflector section; the fuel bundle; an upper trifluted reflector section; and a fuel-handling fixture. A complete subassembly is shown at the bottom of Fig. 2.

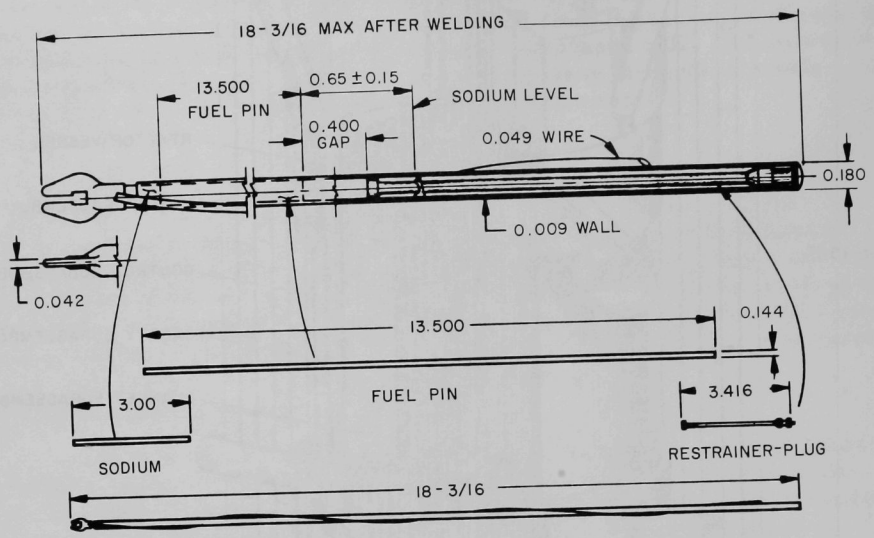

Fig. 2. EBR-II Mark-IA Fuel Element and Subassembly (all dimensions in inches). ANL Neg. No. 103-J5808 Rev. 1.

C. Control and Safety Rods

The hexagonal tube of each control and safety rod has a 0.040-in.-thick wall and measures 1.908 in. across the external flats. Each contains a hexagonally pitched bundle of 61 standard Mark-IA driver-fuel elements. Both the control and the safety rods move vertically in hexagonal thimbles that have the same cross-sectional dimensions as a standard driver subassembly. Although the maximum complement of control and safety rods consists of twelve and two, respectively, two control-rod locations are usually occupied by an instrumented subassembly and a special drop rod for kinetics experiments.

D. Driver-fuel Elements

A standard driver element consists of a 13.50-in.-long, 0.144-in.-dia pin of uranium-5 wt % fissium alloy enriched to 52.2 wt % ^{235}U. The pin is contained in a Type 304 stainless steel jacket, or cladding, having an outside diameter of 0.174 in. and an inside diameter of 0.156 in. A sodium bond, which occupies the annulus separating the fuel material and cladding, serves as a heat-transfer medium. Details of a typical driver element are shown in Fig. 2. Under room conditions (STP), the level of the sodium bond is nominally 0.65 ± 0.15 in. above the fuel material. Above the sodium is a gas reservoir, approximately 0.663 ml in volume, filled with argon. As burnup proceeds and the fuel material swells, bond sodium is displaced upward from the annulus and compresses the argon filling gas.

III. FISSION-PRODUCT MONITORING SYSTEMS

Three on-line fission-product monitors are used at EBR-II for annunciating the release of fission products. One, the fission-gas monitor (FGM), senses the presence of relatively short-lived krypton and xenon fission products in the argon cover gas.[3-5] A second system, the fuel-element rupture detector (FERD), senses the activities of delayed-neutron-emitting species in a bypass stream of primary coolant.[5-7] The third system, the reactor cover-gas monitor (RCGM), consists of three single-channel gamma pulse-height analyzers that monitor the cover gas and register activity levels for the rare-gas fission products ^{133}Xe, ^{135}Xe, and ^{85m}Kr.[5,8]

Two other monitoring techniques, both off-line, are used on a periodic basis.[5] In one, 10-ml samples of cover gas are periodically assayed for ^{133}Xe and ^{135}Xe (approximately six samples per day). In the other, 10-g samples of primary coolant are radiochemically analyzed for ^{137}Cs and ^{131}I on a weekly basis and, whenever a cladding failure is suspected, for ^{133}I and ^{135}I.

Frequent reference to each fission-product monitoring technique will be made throughout the remainder of this report. Although a detailed knowledge of each of the techniques would be beneficial, all that is really necessary in subsequent discussions is an understanding of the type of information provided by the systems and techniques.

During operation of the reactor, fission products continuously recoil from the surface of the fuel into the sodium bond. At any given time, then, the entire spectrum of fission products will be present in the sodium bond. Insofar as annunciation and diagnostic techniques are concerned, only the halogen fission products, bromine and iodine, are of interest. Both species react chemically with the sodium to form the respective bromides and iodides. Of the many bromine and iodine fission products, at least seven are reported to be delayed-neutron emitters. Half-lives for these species range from 0.43 to 55.6 sec.

In the event of a cladding failure that permits the loss of sodium bond, delayed-neutron-emitting species will be swept along with the sodium bond into the flowing coolant stream. If the bond release rate is sufficiently high, the presence of delayed-neutron emitters in the primary coolant will be sensed by the FERD system. If the release rate is low, however, the instantaneous concentration of delayed-neutron-emitting species at the FERD detection point may be too low for detection. Under these conditions, the FERD system would fail to annunciate a release.

However, three of the delayed-neutron emitters, viz., ^{88}Br, ^{89}Br, and ^{138}I, would eventually be sensed by the FGM through their alkali-metal

granddaughters, ^{88}Rb, ^{89}Rb, and ^{138}Cs. In one sense, then, the FERD and FGM systems are redundant in that both rely on common ancestral species.

On the other hand, ^{88}Br, ^{89}Br, and ^{138}I decay continuously in the sodium bond, and their daughters, ^{88}Kr, ^{89}Kr, and ^{138}Xe, diffuse upward through the bond to the gas region of the fuel element. In the event of a defect that permits only the release of gaseous species, ^{88}Kr, ^{89}Kr, and ^{138}Xe (along with other rare-gas fission products) will enter the primary sodium. Within a matter of minutes these will enter the reactor cover-gas plenum and be sensed by the FGM. Thus, any release involving the significant loss of sodium bond will always be sensed by the FGM, but may be missed by the FERD. If the release is fast enough, both systems will respond. It follows, then, that the behaviors of the FERD and FGM systems provide valuable inferential information relating to the rate of bond release.

A similar situation exists for information provided by the RCGM and "grab-sample" analyses, both of which rely on measurements of the ^{133}Xe and ^{135}Xe activities in the reactor cover-gas plenum. The parents of these species, ^{133}I and ^{135}I, are either continuously released or born (from the respective tellurium parents) in the sodium bond. If sodium bond is released through a defect, ^{133}I and ^{135}I will be carried into the primary coolant. The daughters, ^{133}Xe and ^{135}Xe, will eventually be sensed both by the RCGM and through the analysis of cover-gas grab samples. In this case, the signals will follow a buildup curve that is characteristic of the parent and daughter half-lives. In other words, the signal increases will be relatively slow and continuous, and the signal amplitude will either achieve equilibrium or pass slowly through a maximum.

If, on the other hand, the cladding defect permits the release of gases only, the release will still be sensed by the RCGM and grab-sample analyses. In this case, however, the signal increase will be sharp and discontinuous. Even though the reactor continues to operate, the signal will begin to decrease shortly after the releases. Thus, the time-dependent behaviors of both ^{133}Xe and ^{135}Xe can be used to differentiate between bond-type and gas-type releases.

Valuable additional information may be derived from the results of analyses conducted on primary-coolant samples for ^{131}I. Step-type changes in the concentration of ^{131}I can be interpreted in terms of the amount of sodium-bond loss. Similarly, gradual and continuous increases in the ^{131}I content indicate the continuous release of sodium bond through, presumably, a relatively small defect.

Clearly, a degree of redundancy is evident in the information provided by the various techniques. Nevertheless, the fact that information

derived from each method differs with respect to time can be used to advantage, as will be evident in subsequent discussions, in diagnosing specific types of fission-product releases.

Of the five techniques, three serve the dual purposes of annunciation and diagnosis. These are, in the order of increasing response time, the FERD, RCGM, and FGM. The results of calculations based on the volume of the FERD loop and the pumped flow rate indicate a travel time of approximately 17-18 sec between the core and the detection point. Both the RCGM and the FGM monitor activities in a common pumped cover-gas loop, but because of the volume associated with the sodium-vapor de-entrainment traps, the response times of both systems are considerably slower than that of the FERD. Furthermore, a few minutes are needed for the de-entrainment of gas bubbles from the primary sodium and for mixing in the cover-gas plenum. The time required for a given parcel of gas to negotiate the various vapor traps and enter the RCGM detection chamber has been estimated by Brunson to be approximately $2\frac{1}{2}$ min.[8] A similar lag would be experienced by the FGM. The time required for rare-gas species to leave the primary sodium and enter the gas phase is difficult to establish, but an approximate value can be deduced from studies conducted by Smith et al.[5] In these studies, a control rod containing two completely unclad driver-fuel elements was raised from its lowermost to its fully inserted position. Approximately 5-10 min later, a perceptible increase was noted in the signal from the FGM. Assuming $2\frac{1}{2}$ min as the delay associated with the gas line, the time required for rare-gas species to leave the primary coolant and to diffuse throughout the cover-gas system would be very approximately 5 min.

Although the time required for the transit of gas from the cover-gas plenum to the RCGM and FGM detection points is approximately the same, the response time of the RCGM is significantly shorter than that of the FGM. The RCGM operates on a differential principle; i.e., it responds to instantaneous changes in activity levels. The FGM, on the other hand, operates on an integral basis. Alkali-metal species are fixed on a moving wire and stripped in the water layer of a downstream mercury trap. Accordingly, the activity level in the water layer builds up at a rate that depends on the half-lives of the various alkali-metal species. In the rest of this report, it will be assumed that the response time of the RCGM is approximately 5 min and that of the FGM is 5-10 min. In other words, gas activities either released to or born in the primary coolant are sensed approximately 5 min later by the RCGM and 5-10 min later by the FGM.

Although information provided by routine radiometric analyses of cover-gas grab samples is redundant with respect to that from the RCGM, its importance cannot be minimized. Such information has been shown to be accurate, reliable, and reproducible over a period of years. Where sophisticated diagnostic efforts are needed, the information provided by the grab-sample method is preferred to that from the RCGM.

IV. ACTIVITY RELEASES TO THE PRIMARY SYSTEM FROM DRIVER-FUEL ELEMENTS

A. Pressure Buildup in Fuel-element Plenum

From the time a fuel element is assembled into a subassembly (before its insertion into the reactor tank) to the time of its removal from the tank, four sets of conditions act to increase the pressure in the plenum. First is the pressure increase caused by preheating the subassembly in the fuel-unloading machine and the subsequent immersion in the 700°F primary coolant. The gas pressure increases from a nominal value of 14.7 psi (for fuel fabricated at sea level) to 32.2 psi. After the subassembly is installed in the core, a second pressure increase results when the reactor is taken to power. Assuming a nominal coolant-outlet temperature of 883°F, the pressure will increase from 32.2 to 37.2 psi. (Upon shutdown, the pressure will of course revert to 32.2 psi, assuming the absence of physical changes during the operation.)

With the reactor operating at power, two other, internal, effects act to increase the pressure above the nominal pressure of 37.2 psi. One is related to density changes in the fuel, and the other to the direct release of rare-gas fission products.

1. Pressure Increase from Fuel-density Changes

As the fuel material "burns," its volume increases both radially and axially. Since the metallic matrix is essentially impervious, the sodium bond is forced from the annulus to the plenum at the top of the element. The already pressurized filling gas becomes further compressed. The extent of fuel swelling depends on the following variables: fuel composition, operating temperature, and burnup. For fuel material burned to a normal level of 1.8 at. %, volumetric expansion ($\Delta V/V$) may vary from 11% for low-swelling (high-silicon content) fuel to as much as 16% for high-swelling (low-silicon) material.[9,10] From the information and calculational methods described by Henault,[11] the gas pressure in a low-swelling element at 1.8 at. % burnup, assuming a $\Delta V/V$ of 11%, would be 150 psia. For high-swelling fuel material, the gas pressure would be 2900 psia. Both of the above values are based on 62.5-MWt operating conditions, a gas-plenum temperature of 1025°F, and a maximum sodium-bond inventory. In both cases, differential expansion effects in fuel, cladding, and sodium bond were considered. It was also assumed that the contribution to gas pressure from rare-gas accumulation was negligible. As will be shown in the following paragraph, this component is indeed very small.

2. Pressure Increase from the Direct Release of Rare-gas Fission Products from the Fuel

The principal origin of rare-gas fission products in the gas plenum is the recoil release of the respective halogen parents, i.e., bromine

and iodine. Since the independent fission yields for all rare-gas fission-product isotopes are negligible, the inventory of krypton and xenon isotopes in the plenum essentially originates from the simple beta decay of the respective halogen parents. Because the effective range of fission fragments in uranium-fissium fuel is extremely small, i.e., a few tenths of a mil, only a minute fraction of the fission-product inventory in the fuel material appears in the bond or the gas plenum. According to coauthor E. R. Ebersole, who has measured the ^{131}I inventories in both the fuel material and sodium bond, the fraction of fission products that leaves the fuel matrix is only 0.05%. Assuming that 28% of all fission products eventually decay to stable rare-gas isotopes, it is a simple matter to show that the volume (STP) of rare-gas species in the plenum of a driver element with a burnup of 1.8 at. % is only 0.013 cm^3. Since the original volume (STP) was 0.663 cm^3, the effect of recoil release of rare-gas fission products to the gas plenum is insignificant.

Although the pressure in a driver element does indeed increase as it is irradiated to its target burnup, the volume of the gas decreases. As discussed in Sec. IV.C, this fact must be carefully considered in evaluating the extent to which sodium bond may be lost in the event of a cladding defect. As background for subsequent discussions, attention will be directed to two specific types of defects. These will be categorized according to the location of the defect, i.e., whether the defect occurs above or below the top of the fuel material.

B. Cladding Defects above Fuel Elevation

If the defect is in the region of the upper weld, the argon filling gas, along with stable and radioactive noble-gas fission products, will leak to the primary system. For this type of defect, the sodium bond in the annulus between the fuel and cladding will remain undisturbed.

If, on the other hand, the defect is located between the top of the fuel column and the sodium-bond level, the relatively high gas pressure (relative to the combined static and dynamic primary-coolant pressure at that point) will force sodium bond through the defect. It follows that once the bond level reaches the defect level, filling gases may also leak through the defect. If filling gas is lost, a subsequent reactor shutdown and startup can actually lead to an increase in the sodium inventory of the element. All fuel elements in the core experience two external pressure components: one from the static head of sodium, approximately 6 psig, and the other from the primary-coolant pumps. The latter component is variable and depends not only on axial elevation but on the row in which the element is located. The pressure component associated with the pumped coolant flow ranges from a high of 34.8 psig at the bottom of an element in row 1 or 2 to a low of 7.1 psig at the top of an element in row 6.

If filling gas is lost under operating conditions, an additional amount can be lost when the primary pumps are turned off at the next shutdown. During the following startup, when the pumps are turned on, sodium from the primary system will be forced inward through the defect. Because the original gas inventory was reduced, the new sodium level will be between the defect and the top of the fuel element.

If the defect is large, sodium can be intermittently exchanged between the element and the primary coolant system. The sodium pressure at the defect will be continually changing. For a brief period (seconds or less), the pressure gradient may be such that sodium leaves the element. For a following period, the gradient may reverse and sodium may flow inward through the defect. In a very real sense, such a mechanism resembles a check valve which permits the net outward flow of iodine-rich sodium bond. (For the inward portion of the cycle, the sodium is deficient in iodine species.) An actual case illustrating these considerations is discussed in detail in Sec. VI. The important consideration is that if a defect develops above the fuel elevation, fuel material cannot become exposed. Fission products can, however, leave the element, but these in no way affect the safe continued operation of the system.

C. Cladding Defects below Fuel Elevation

Clearly, cladding defects that develop along the length of the fuel column can lead to loss of sodium bond through the defect. At various times, considerable concern has been expressed about the possibility of uncovering and melting fuel material. Although this possibility still exists, it is now known that several forces and several actions combine to minimize deleterious effects. In fact, just how such forces and actions affect the consequences of sodium-bond loss constitutes the principal subject of this report.

First of all, a cladding defect anywhere along the length of the fuel may not necessarily lead to fuel unbonding. Because the dynamic pressure exerted by the flowing sodium varies both axially and radially throughout the core, the extent of fuel unbonding associated with a cladding failure depends on the location of the element and the defect. The extent of fuel unbonding also depends on the following factors: the filling pressure of the element, the type of fuel material, the fuel burnup, and the initial level of the bond sodium. It is instructive, then, to consider the maximum extent of fuel unbonding that may credibly be encountered in the normal operation of EBR-II. In his evaluations of fuel unbonding, Henault[11] assumed the following as a worst case: (1) a low-swelling (high-silicon) Mark-IA fuel element, (2) a burnup of 1.8 at. %, (3) a defect located at the lower weld, (4) a filling pressure of 14.7 psi, and (5) a low sodium level (0.50 in. above the fuel column). Using these assumptions, Henault found that regardless of element location in rows 1-3, fuel unbonding would not occur. Limited unbonding

would occur in row 4 and would become progressively worse for more outlying locations. For example, in row 4 as much as 2.4 in. of fuel could be uncovered; in row 5, 6.0 in.; and in row 6, 8.0 in. Thus, defects in the region of the lower weld (and these are the most likely) may not necessarily lead to fuel unbonding.

In Sec. VII of this report, it is shown that even if unbonding should occur, the consequences would not be particularly serious.

V. FISSION-PRODUCT RELEASE DIAGNOSTICS

A. Intercalibration of Monitoring Systems

One of the most vital items of information needed in diagnosing the nature of a given activity release to the primary system is the response of the various fission-product monitoring systems to the hypothetical complete release of all fission products in the bond and gas plenum of a driver element. Experimental measurements of the maximum expected response have been made by measuring the various responses when two completely unclad driver-fuel pins were deliberately irradiated in the core.[5] Under normal operating conditions, i.e., with no exposed fuel, the entire spectrum of fission products is continuously generated from fissions in fuel material that exists as an unavoidable contamination on the surfaces of core components. Fission products generated in this manner are sensed by the various monitoring systems as an ever-present background or noise component.

When unclad fuel material is deliberately inserted in the core, fission products recoil from the surface. Delayed-neutron-emitting species generated in this manner are almost immediately sensed by the FERD system; the rare-gas species accumulate in the cover-gas plenum, where they are eventually sensed by the RCGM and FGM systems. If the unavoidable background for a given index species is defined as noise and the component generated from the exposed fuel as signal, it can be shown that the signal-to-noise (S/N) ratio for all index species (regardless of monitoring technique) will be the same when the principal release mechanism is recoil-based. Furthermore, the S/N ratio will be independent of the power history. In establishing upper limits for the S/N ratio for a single driver element, it is immaterial whether a given index species recoils directly into the coolant or whether it accumulates in the bond and gas plenum of an intact fuel element that subsequently releases the entire bond and gas inventory to the primary system through a defect. The S/N ratio (at equilibrium) will be the same for both cases.

To measure the maximum signal that conceivably could originate from a single driver-fuel element, two completely unclad fuel pins were irradiated in a control rod (row 5). From measurements of the equilibrium noise component made before the installation of the exposed fuel, and the equilibrium signal after the installation, a single-pin S/N ratio of 4.0 was established.[5] Through the use of empirical data for axial and radial power profiles, the corresponding value for an unclad fuel element in a row-1 position was found to be approximately 5.0.

This information alone has proved valuable in diagnosing the nature and origin of inadvertent activity releases to the primary system (ARP's).

On several occasions, measurements of the S/N ratio for an inadvertent ARP from an unidentified element have been used to eliminate driver-fuel elements from suspicion. On those occasions when S/N ratios significantly larger than 5.0 were measured, it was assumed that a single driver element could not be involved, since the loss of the entire bond and gas inventory could not account for the strength of the signal. In such cases, the elimination of driver fuel narrowed the search to experimental ceramic-fuel elements, which can release significantly higher fractions of their rare-gas fission-product inventories to the primary system.

B. Differentiation between Gas-type and Bond-type Releases

1. Gas-type Releases

In the event of an ARP, valuable diagnostic information can be inferred from the individual responses of the various monitoring systems. Because the FERD system is sensitive to the presence of delayed-neutron emitters in the primary coolant, its response in the event of a cladding defect provides considerable insight into the type of defect. In the event of a gas-type ARP in either a driver-fuel element or an experimental irradiation capsule, krypton and xenon fission products will be released to the coolant and will ultimately diffuse upward to the cover-gas plenum. Eventually the increased activity levels for rare-gas species will be sensed by the RCGM, and in most instances by the FGM. Delayed-neutron-emitting species, presumably bromine and iodine, remain chemically fixed in the bond, which remains undisturbed. The FERD system, then, will fail to annunciate a gas-type release.

If the FGM responds, increases will also be sensed by the RCGM and indicated by radiometric analyses conducted periodically on cover-gas samples for ^{133}Xe and ^{135}Xe. Fundamental to this argument is the fact that if ^{88}Kr, ^{89}Kr, and ^{138}Xe (all short-lived index species for the FGM) are released from the element or capsule, either as gases or as the result of decay from the respective halogen parents, ^{133}Xe and ^{135}Xe will also be released. The converse, however, is not necessarily true. If, for example, the RCGM registers increases for ^{133}Xe and ^{135}Xe and the increases are confirmed by cover-gas analyses for these species, the FGM may or may not respond, depending on the nature of the defect. If the defect is associated with an encapsulated fuel element, it is conceivable that the release of fission-product gases to the primary system may have followed an earlier release from the encapsulated fuel element to the capsule. If the time between the two releases is long compared with the half-lives of the FGM index species, such species will have decayed before the secondary release. In other words, the gas released to the system may be highly fractionated in favor of the long-lived rare-gas species. Such behavior is not conjectural; several examples of extreme fractionation phenomena have actually been observed, and in all cases, the release was

ultimately identified with an encapsulated fuel specimen. The absence of encapsulation for driver-fuel elements eliminates the possibility of corresponding fractionation effects for driver elements. Accordingly, whenever extreme fractionation phenomena accompany a gas-type release, encapsulated fuel elements are considered prime suspects.

2. Bond-type Releases

For a bond-type ARP, chemically fixed iodine and bromine fission products extrude with the bond and, on subsequent decay, lead to the generation of krypton and xenon isotopes, which eventually diffuse upward into the cover-gas plenum. Cursorily, it would seem that the loss of sodium bond would eventually be sensed by the FERD, RCGM, FGM, and radiometric analyses, since the ancestors of all index species for these systems are halogens. Care must be taken, however, to consider the rate of bond release. If the rate of release is relatively fast (i.e., a substantial fraction of the bond inventory is lost over a period of seconds or minutes), all systems, including the FERD, will register increases. If, on the other hand, the release of bond sodium to the coolant occurs over a period of hours or days, the release rate of delayed-neutron emitters may be smaller than the generation rate of delayed-neutron emitters from background sources and is not likely to be annunciated by the FERD system.

The migration and diffusion of delayed-neutron-emitting species in the bond must also be considered. If bond is slowly being extruded from a defect in the cladding above the fuel but below the sodium level, only a very small fraction of the total delayed-neutron-emitter inventory will negotiate the path from the place of recoil birth through the bond to the defect. In such cases, even the FGM will fail to respond, since the index species for the FGM are the daughters of the delayed-neutron-emitting index species for the FERD. On the other hand, the longer-lived iodine species such as ^{133}I and ^{135}I live long enough to diffuse throughout the bond and, upon extrusion with the bond, give rise to the respective xenon-daughter activities.

In all cases of bond extrusion, regardless of the size of the defect, the release of ^{133}I and ^{135}I (chemically fixed in the bond) to the primary coolant is sensed by the RCGM as additional sources of ^{133}Xe and ^{135}Xe. Accordingly, each of these activities will give rise to secondary buildup curves which are superimposed on the ^{133}Xe and ^{135}Xe buildup curves obtained from background sources. For both isotopes, of course, the amplitudes and time dependencies of the secondary buildup curves depend on the size of the defect and the half-lives of the respective I-Xe fission-product pairs.

On several occasions when a defect has been suspected, valuable diagnostic information has been generated by shutting the reactor

down and turning off the primary coolant pumps. When the pumps are turned off, the consequent pressure reduction at defect elevation may be sufficient to cause the release of sodium bond if the defect is below the sodium level. Similarly, the reduction in pressure may cause an expansion of fission-product and argon-fill gas through the defect if the defect is located above the sodium level.

When the nature of a failure is diagnosed, care must be taken to differentiate between the two types of fractionation phenomena discussed above. In one case, fractionation involves a delay between an initial and secondary gas release from an encapsulated element. In the other case, fractionation involves the inability of short-lived halogen species to negotiate the path from recoil birth to extrusion through a defect. To differentiate between these possibilities, analyses are conducted for ^{131}I and ^{133}I in coolant samples collected before and after the failure. For the first case, no increase in the concentrations of iodine index species in the coolant will be found. In the second case, an increase is regarded as conclusive evidence that the release involves the extrusion of bond sodium.

VI. MATHEMATICAL CONSIDERATIONS FOR LOSS-OF-BOND-TYPE DEFECTS

A. Mechanisms for Sodium-bond Loss

Under normal operating conditions, the sodium bond in any given driver-fuel element contains halogen fission products in the form of sodium halides. If a cladding defect in the fuel region develops, sodium bond, along with fission-product halides, can be driven out through the defect into the flowing primary sodium. Subsequent decay of the halides results in the formation of the respective rare-gas daughters.

If the extrusion takes place over a short period of time, i.e., minutes or less, the activities of the rare-gas daughters in the cover gas will build up and decay according to the half-lives of the parent-daughter pairs. The activity curve established by the RCGM and analyses of cover-gas samples will indicate a gradual buildup to a peak and eventually a decay back to the original background level. Furthermore, the peak will be delayed relative to the initial loss of bond by a precise interval, which depends only on the half-lives of the parent-daughter pair. For the $^{135}I/^{135}Xe$ pair, the peak will occur 11.6 hr after the bond loss, regardless of whether the reactor continues to run or is shut down.

If the bond extrusion takes place over a longer period, hours for example, the buildup of rare-gas species in the cover-gas plenum will follow a different time dependence. Because the bond is being extruded at a slower rate, the buildup of rare-gas daughters will take place over a longer period. Assuming the reactor continues to run and assuming that the bond extrusion process eventually ceases, as it should, more time will be required for cover-gas activities to reach their peak. In principle, then, the shape of the buildup curve, and the time of occurrence of the peak, depend on the rate of bond loss.

Whether the reactor continues to run or is shut down has little to do with such observations. A pulse-type bond release would still be observed as a precisely defined peaking of cover-gas activities. Similarly, a gradual bond release would be manifested in the form of a peak delayed in time by an amount that depends on the leak rate.

One other case of bond loss is worthy of recognition. If conditions are such that bond sodium is intermittently and indefinitely exchanged with the primary sodium, the emission of iodine species will appear as an additional source superimposed on the normal background level. Under such circumstances, the activity levels of rare-gas daughters in the cover gas will be higher than normal and will follow a buildup-to-equilibrium behavior similar to that of the normal background. In this case, peaking will not be observed. If FERD and FGM information were not available, such

behavior could easily be attributed to an increase in the contamination level of fuel-element surfaces. However, FERD and FGM information is always available, and under the conditions described above would indicate no change in the equilibrium background level. The possibility of intermittent exchange of bond sodium with primary coolant is more than conjectural. Such behavior has been observed on two separate occasions. On those occasions, as described in more detail in Sec. VIII, the behaviors of rare-gas species in the cover gas were completely in accord with the considerations discussed above.

B. Mathematical Considerations

Considerable success has been achieved in effecting a consistency between the observed fission-product behaviors under inadvertent release conditions and those expected from relatively straightforward physical-mathematical models. In diagnosing the nature of bond-type releases from EBR-II driver-fuel elements, seven specific cases are of interest. These are:

Case 1: Normal (tramp) background, assuming a rapid increase to power and a rapid shutdown from power.

Case 2: Normal (tramp) background, assuming a normal increase to power and a normal shutdown from power.

Case 3: Slow loss of bond under operating conditions; leak develops during reactor startup.

Case 4: Pulse-type loss of bond under operating conditions; leak develops under conditions of radioactive equilibrium.

Case 5: Slow loss of bond under operating conditions; leak develops under conditions of radioactive equilibrium.

Case 6: Slow loss of bond, followed by reactor and primary-pump shutdown.

Case 7: Rapid loss of bond, followed by reactor and primary-pump shutdown.

Mathematical expressions for the seven cases are derived below. For simplicity, the various developments are limited to the $^{135}I/^{135}Xe$ pair. Application to any other halogen-rare-gas pair can be made by a simple change of subscript and the use of the proper half-lives. To illustrate the qualitative behavior of rare-gas fission products for each type of bond release, arbitrary but realistic conditions have been assumed. In effect, the illustrations provide "fingerprint" sets for the various types of release. The agreement between the behaviors indicated by the fingerprint sets and those observed under inadvertent release conditions is also illustrated below.

1. Case 1. Normal (Tramp) Background, Assuming a Rapid Increase to Power and a Rapid Shutdown from Power

In the following mathematical developments, two assumptions are made: (1) The reactor starts from a cold, clean condition; i.e., background levels are negligible; and (2) the reactor is brought to power over a period of time much shorter than the half-lives of the $^{135}I/^{135}Xe$ fission-product pair. In practice, neither of these, particularly condition (2), applies. Nevertheless, the development is instructive, and the effects of a normal startup are considered in a subsequent example.

The differential equation for the rate of change of the number of ^{135}I atoms in the primary system at any given time is

$$\frac{dN_{1T}}{dt} = Q_T - \lambda_1 N_{1T}, \tag{1}$$

where N_{1T} is the number of atoms of ^{135}I, t is the time (sec) after reactor startup, λ_1 is the decay constant of the N_1 species (sec^{-1}), and Q_T is the generation rate (atoms/sec) of ^{135}I from fissions in tramp uranium, i.e., surface contamination of the fuel elements with fuel material. In this and all subsequent developments, the subscript T refers to tramp origin. Upon integration, Eq. 1 becomes

$$N_{1T} = \frac{Q_T}{\lambda_1}[1 - \exp(-\lambda_1 t)]. \tag{2}$$

The rate of change of ^{135}Xe atoms originating from the decay of ^{135}I is given by

$$\frac{dN_{2T}}{dt} = \lambda_1 N_{1T} - \lambda_2 N_{2T}, \tag{3}$$

where N_{2T} is the number of atoms of ^{135}Xe at any time t, and λ_2 is the respective radioactive decay constant. Inserting N_{1T} from Eq. 2 into Eq. 3 gives

$$\frac{dN_{2T}}{dt} = Q_t[1 - \exp(-\lambda_1 t)] - \lambda_2 N_{2T}. \tag{4}$$

Integration of Eq. 4 gives

$$N_{2T} = \frac{Q_T}{\lambda_2(\lambda_1 - \lambda_2)}\{\lambda_1[1 - \exp(-\lambda_2 t)] - \lambda_2[1 - \exp(-\lambda_1 t)]\}. \tag{5}$$

At equilibrium, i.e., after the reactor has operated for a long time compared to the half-lives of the $^{135}I/^{135}Xe$ pair, Eq. 5 reduces to

$$N_2T = \frac{Q_T}{\lambda_2}.$$

Hence, the activity of ^{135}Xe, i.e., $\lambda_2 N_2 T$, will be the same as the source term, Q_T.

When the reactor is shut down, the source term Q_T vanishes and the ^{135}Xe immediately begins to decay. In the development given below, it is assumed that the power level is decreased rapidly to zero. The refinements needed to account for a gradual (usual) shutdown are considered in Case 2 (below).

At the instant of shutdown, the inventory of ^{135}Xe in the primary system begins to decay. However, the ^{135}I generated during the power operation is also present and continues to produce ^{135}Xe at a decreasing rate after the shutdown. Equation 5, which gives the number of atoms of ^{135}Xe present at any given time t after startup, can be modified to give the ^{135}Xe activity at any given time T after the shutdown. Thus,

$$\text{Activity of } ^{135}Xe = \lambda_2 N_2 T = \frac{Q_T \exp(-\lambda_2 T)}{\lambda_1 - \lambda_2}\{\lambda_1[1 - \exp(-\lambda_1 t)] - \lambda_2[1 - \exp(-\lambda_2 t)]\}. \tag{6}$$

The ^{135}Xe component that originates from the ^{135}I content of the primary system at shutdown can be found from Eq. 2. The disintegration rate of ^{135}I at any given time T after shutdown is

$$\lambda_1 N_1 T = Q_T[1 - \exp(-\lambda_1 t)] \exp(-\lambda_1 T), \tag{7}$$

and the buildup rate of ^{135}Xe from this component is

$$\frac{dN_2T}{dt} = Q_T[1 - \exp(-\lambda_1 t)] \exp(-\lambda_1 T) - \lambda_2 N_2 T. \tag{8}$$

Because of the definition of T, the parameter t in Eqs. 6-8 is a constant, the irradiation time in seconds. T, then, is a variable in Eqs. 6-8, the time after shutdown in seconds.

With integration, Eq. 8 becomes

$$\lambda_2 N_2 T = \frac{Q_T[1 - \exp(-\lambda_1 t)]\,\lambda_2}{\lambda_2 - \lambda_1}[\exp(-\lambda_1 T) - \exp(-\lambda_2 T)]. \tag{9}$$

The activity of ^{135}Xe following the shutdown is simply the sum of the two components given by Eqs. 6 and 9.

An illustration of the startup and shutdown behavior of ^{135}Xe in the primary system under the assumptions cited above is given in Fig. 3. In the case illustrated, the conditions assumed are: an equilibrium ^{135}Xe activity of 3.0×10^{-3} μCi/ml, and a total uninterrupted irradiation of 5.5 days.

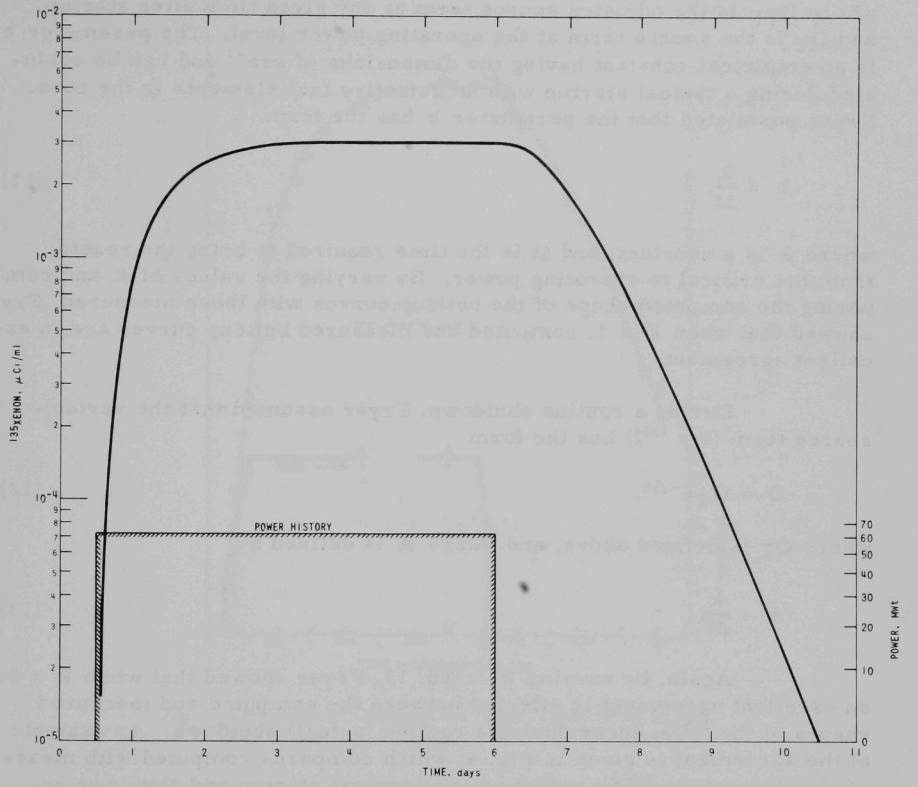

Fig. 3. Startup and Shutdown Behavior of Tramp ^{135}Xe; Startup and Shutdown Periods Short Compared to Half-lives

2. Case 2. Normal (Tramp) Background, Assuming a Normal Increase to Power and a Normal Shutdown from Power

In practice, normal reactor startups and shutdowns take place over about 10 hr. During this period, the power level is changed incrementally, and the assumption of the constant source term Q_T in the expressions above is invalid. Fryer[12] has considered the effects of a varying power level during startups and shutdowns, and has established an empirical and practical

method that can be used to account for the power changes. To correct for the time-dependent change in Q_T during startup, Fryer assumed that Q_T follows a dependence given by

$$Q_{TP} = Q_T(1 - e^{-bt}), \tag{10}$$

where Q_{TP} is the adjusted source term at any given time after startup, and Q_T is the source term at the operating power level. The parameter b is an empirical constant having the dimensions of sec^{-1} and can be evaluated during a typical startup with no defective fuel elements in the core. Fryer postulated that the parameter b has the form

$$b = \frac{k}{\Delta t}, \tag{11}$$

where k is a constant, and Δt is the time required to bring the reactor from hot critical to operating power. By varying the values of k and comparing the computed shape of the buildup curves with those measured, Fryer showed that when k = 1, computed and measured buildup curves are in excellent agreement.

During a routine shutdown, Fryer assumed that the variable source term (for ^{135}I) has the form

$$Q = Q_T e^{-At}, \tag{12}$$

where Q_T is defined above, and where A is defined by

$$A = \frac{k}{\Delta t}. \tag{13}$$

Again, by varying k in Eq. 13, Fryer showed that when k = 0.8 an excellent agreement is effected between the computed and measured shapes of the ^{135}Xe decay during a routine (actual) shutdown. An example of the agreement is given in Fig. 4, which compares computed with measured values of the ^{135}Xe activity during typical startup and shutdown regimes. Clearly, the agreement is excellent.

The significance of the ability to predict the exact shape and amplitude of the tramp ^{135}Xe buildup and decay curves cannot be overemphasized. For any given run and any given set of power-time conditions, the tramp ^{135}Xe activity can be accurately predicted. Hence, any deviation from the computed behavior can be directly attributed to the release of fission products from a defective fuel element. Subtraction of computed values from measured values defines the component associated with the release. As will become evident from the development that follows below,

the amplitude and time dependence of the separated (leakage) component can be used to provide valuable insight into the nature and origin of the release.

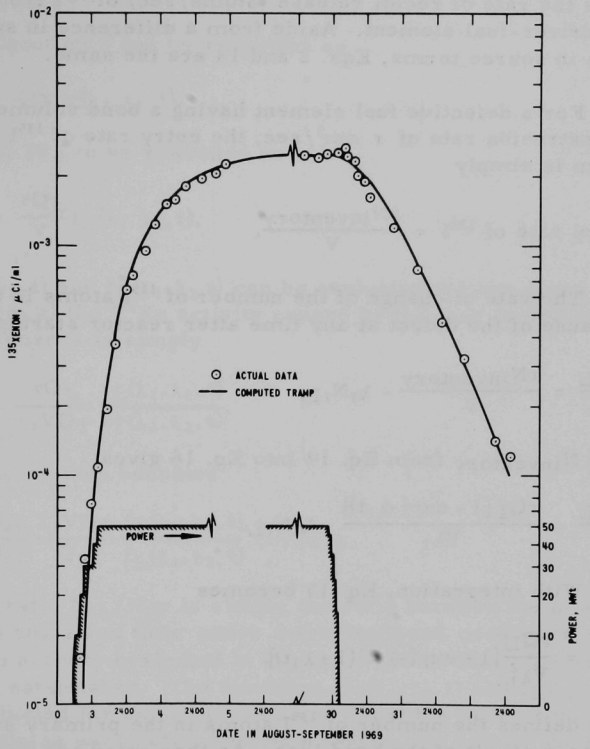

Fig. 4. Comparison of Computed and Actual Tramp ^{135}Xe for the Startup and Shutdown of Run 37. ANL Neg. No. 103-M5651.

3. Case 3. Slow Loss of Bond under Operating Conditions; Leak Develops during Reactor Startup

The following development is concerned with the ^{135}Xe activity resulting from the release of bond sodium through a defect in the cladding of a Mark-IA driver-fuel element.

Using the nomenclature defined above for ^{135}I and ^{135}Xe, and defining the recoil release rate of ^{135}I from the surface of the fuel material (in a single element) as Q_L atoms/sec, the number of ^{135}I atoms in the bond of the fuel element at any given time is

$$N_{inventory} = \frac{Q_L}{\lambda_1}[1 - \exp(-\lambda_1 t)], \tag{14}$$

where Q_L is the rate of recoil release (atoms/sec) of ^{135}I from the surface of a single driver-fuel element. Aside from a difference in subscripts and a difference in source terms, Eqs. 2 and 14 are the same.

For a defective fuel element having a bond volume of V cm^3 and a bond extrusion rate of r cm^3/sec, the entry rate of ^{135}I into the primary system is simply

$$\text{Entry rate of } ^{135}I = \frac{rN_{inventory}}{V}. \tag{15}$$

The rate of change of the number of ^{135}I atoms in the primary coolant because of the defect at any time after reactor startup is

$$\frac{dN_1L}{dt} = \frac{rN_{inventory}}{V} - \lambda_1 N_1 L. \tag{16}$$

Substituting $N_{inventory}$ from Eq. 14 into Eq. 16 gives

$$\frac{dN_1L}{dt} = \frac{rQ_L[1 - \exp(-\lambda_1 t)]}{V\lambda_1} - \lambda_1 N_1 L. \tag{17}$$

With integration, Eq. 17 becomes

$$N_1L = \frac{rQ_L}{V\lambda_1^2}[1 - \exp(-\lambda_1 t)(1 + \lambda_1 t)]. \tag{18}$$

Equation 18 defines the number of ^{135}I atoms in the primary system at any given time as a result of the bond loss. As they enter and accumulate in the primary system, the ^{135}I atoms decay to ^{135}Xe. The buildup rate of ^{135}Xe in the primary system is

$$\frac{dN_2L}{dt} = \frac{rQ_L}{V\lambda_1}[1 - \exp(-\lambda_1 t)(1 + \lambda_1 t)] - \lambda_2 N_2 L. \tag{19}$$

With integration, Eq. 19 becomes

$$N_2L = \frac{rQ_L}{\lambda_1\lambda_2 V(\lambda_2 - \lambda_1)^2}\{(\lambda_2 - \lambda_1)^2$$

$$- [\lambda_2(\lambda_2 - \lambda_1) + \lambda_1\lambda_2^2 t - \lambda_1^2\lambda_2 t - \lambda_1\lambda_2] \exp(-\lambda_1 t)$$

$$- [(\lambda_2 - \lambda_1)^2 - \lambda_2(\lambda_2 - \lambda_1) + \lambda_1\lambda_2] \exp(-\lambda_2 t)\}. \tag{20}$$

Equations 5 and 20 can be used to estimate the bond leak rate from an element that develops a leak during startup and maintains the same leak rate after operating power is reached.

Equation 5 can be rewritten as

$$N_2T = Q_T f_T(\lambda_1, \lambda_2, t). \tag{21}$$

Similarly, Eq. 20 can be rewritten as

$$N_2L = \frac{rQ_L}{V} f_L(\lambda_1, \lambda_2, t), \tag{22}$$

where $f_T(\lambda_1, \lambda_2, t)$ and $f_L(\lambda_1, \lambda_2, t)$ can be evaluated for any given value of t. Hence the ratio of the ^{135}Xe activity caused by the leak to that originating from tramp sources is simply

$$\frac{N_2L}{N_2T} = \frac{rQ_L}{\lambda_1 V Q_T} \frac{f_L(\lambda_1, \lambda_2, t)}{f_T(\lambda_1, \lambda_2, t)}. \tag{23}$$

The leak rate, r, then becomes

$$r = \frac{N_2L}{N_2T} \frac{\lambda_1 V Q_T}{Q_L} \frac{f_T(\lambda_1, \lambda_2, t)}{f_L(\lambda_1, \lambda_2, t)} \text{ cm}^3/\text{sec}. \tag{24}$$

In Eq. 24 the ratio N_2L/N_2T is simply the ratio between the measured activity of ^{135}Xe at any given time under extruding bond conditions and the normal tramp activity evaluated at the same time. Thus, the ratio N_2L/N_2T can easily be established. The functions, $f_T(\lambda_1, \lambda_2, t)$ and $f_L(\lambda_1, \lambda_2, t)$ can easily be evaluated for any given value of t and the decay constants λ_1 and λ_2. The remaining parameter, the ratio Q_T/Q_L, is simply the reciprocal of the S/N ratio measured under exposed-fuel conditions.[5] Because the latter statement may not be intuitively clear, the reader is reminded that Q_T is defined as the rate of ^{135}I generated from tramp sources, and Q_L is defined as the recoil release rate of ^{135}I from the surface of a completely exposed fuel pin. The ratio of these two release rates is precisely determined in exposed-fuel measurements.

An illustration of the time-dependent ^{135}Xe behavior associated with the type of bond release discussed above is given below. In these calculations, the following conditions are assumed: (1) The cladding defect develops during a routine startup, (2) the release rate of bond sodium is 5.5×10^{-6} cm^3/sec, and (3) the defective fuel element is located in a row-5 position. The calculated results are compared in Fig. 5 with data from an actual bond release of this type. The figure contains three calculated curves: (1) one for normal conditions, i.e., with all driver-fuel elements intact, (2) one for a row-5 element that is extruding sodium bond at a

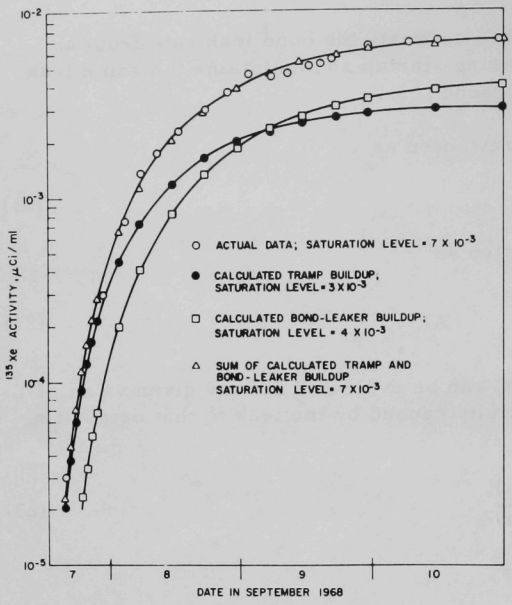

Fig. 5. Buildup Curves for ^{135}Xe Activity, Showing How the Behavior for Tramp ^{135}Xe Differs from That for a Continuous Bond Release. ANL Neg. No. 103-L5184.

rate of 5.5 x 10^{-6} cm^3/sec, and (3) a total of the other two. In comparing the curves, the reader is reminded that the normal buildup curve can be reliably predicted from the equilibrium tramp activity measured in the previous run. Hence, any difference between the measured curve and the predicted curve can be interpreted in terms of the bond release.

Two important features are apparent in comparing the curves of Fig. 5. One, of course, is the higher total under loss-of-bond conditions. The other is a difference in the rate of buildup which, according to Eq. 19, should be slower for the leaker component than for the tramp component. In effect, then, the information illustrated in Fig. 5 constitutes a fingerprint for the behavior of ^{135}Xe in the cover gas when bond sodium extrudes under startup conditions or before the realization of radioactive equilibrium.

4. Case 4. Pulse-type Loss of Bond under Operating Conditions; Leak Develops under Conditions of Radioactive Equilibrium

After the reactor has operated at power long enough for the ^{135}I/^{135}Xe pair to be at equilibrium, the number of ^{135}I atoms in the primary coolant is Q_T/λ_1. The number of ^{135}I atoms in the bond of a given fuel element is Q_L/λ_1. If a defect develops at the lower end of a fuel element, and if the entire bond inventory in the annulus extrudes rapidly, the number of additional ^{135}I atoms in the primary coolant system will be Q_L/λ_1. The disintegration rate of the ^{135}I from tramp origin will be Q_T, and the disintegration rate of the ^{135}I from the expelled bond sodium will be

$$\frac{dN_1L}{dt} = Q_L \exp(-\lambda_1 t). \qquad (25)$$

The differential equation for the buildup and decay of ^{135}Xe from the ^{135}I expelled with the bond is

$$\frac{dN_2L}{dt} = Q_L \exp(-\lambda_1 t) - \lambda_2 N_2L, \tag{26}$$

which, upon integration, becomes

$$N_2L = \frac{Q_L}{\lambda_1 - \lambda_2}[\exp(-\lambda_1 t) - \exp(-\lambda_2 t)]. \tag{27}$$

Hence, the activity of the ^{135}Xe component associated with the bond loss will be

$$\frac{dN_2L}{dt} = \frac{Q_L\lambda_2}{\lambda_1 - \lambda_2}[\exp(-\lambda_1 t) - \exp(-\lambda_2 t)]. \tag{28}$$

The activity level of the ^{135}Xe tramp component will, of course, be simply

$$\frac{dN_2T}{dt} = Q_T. \tag{29}$$

The time behavior of the signal and tramp components, before and after the postulated release, is shown in Fig. 6. Note the peaking of the ^{135}I and the displacement of the peak 11.6 hr after the bond release.

The S/N ratio, for this type of release, is time-dependent and is given by the ratio of Eq. 28 to Eq. 29; hence,

$$\text{S/N ratio} = \frac{Q_L\lambda_2}{Q_T(\lambda_1 - \lambda_2)}[\exp(-\lambda_1 t) - \exp(-\lambda_2 t)]. \tag{30}$$

5. Case 5. Slow Loss of Bond under Operating Conditions; Leak Develops under Conditions of Radioactive Equilibrium

If the reactor has been operating long enough to establish equilibrium for the $^{135}I/^{135}Xe$ pair, and if a very slow bond leak develops, the shape of the buildup curve for ^{135}Xe will differ considerably from that illustrated for Case 3 (Fig. 5). Since the sodium inventory in a driver-fuel element is finite, any continuous leak must eventually cease. On the other hand, as discussed earlier, the intermittent exchange of bond and primary sodium coolant through a defect may be approximated by an effective release rate that is continuous and indefinite.

For illustration in the discussion that follows, the assumption is made that a release rate of r cm^3/sec of bond sodium continues indefinitely. The disintegration rate of ^{135}I in the primary sodium from tramp origin is again

$$\frac{dN_1T}{dt} = Q_T. \tag{31}$$

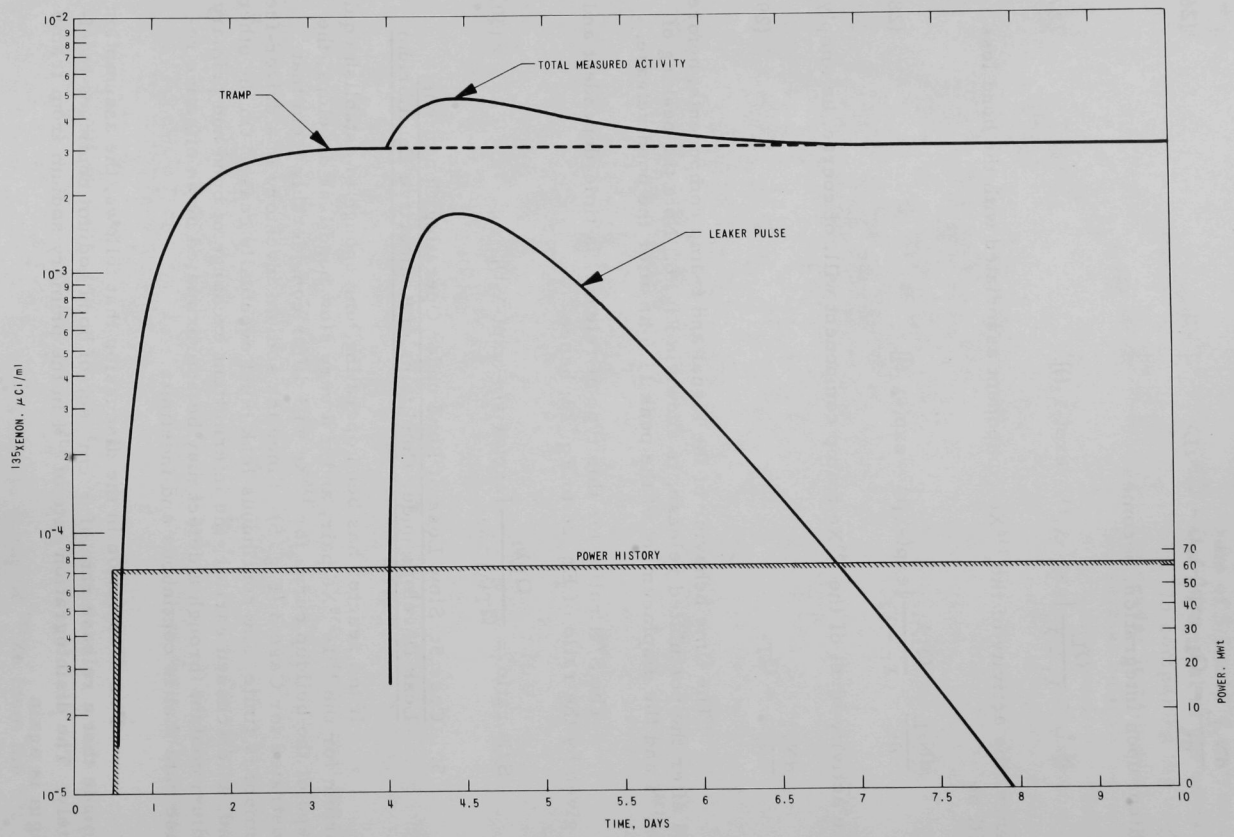

Fig. 6. Xenon-135 Activity Generated by a Pulse-type Loss of Bond under Equilibrium Conditions

The number of atoms of ^{135}I in the annulus of the fuel element is Q_L/λ_1. If a leak develops and continues indefinitely at the rate of r cm^3/sec, the entry rate of ^{135}I atoms from the bond is

$$\text{Entry rate of } ^{135}I \text{ from bond} = \frac{rN_1L}{V} = \frac{rQ_L}{V\lambda_1}. \tag{32}$$

The ^{135}I component in the primary coolant associated with the leak is defined by the differential equation

$$\frac{dN_1L}{dt} = \frac{rQ_L}{V\lambda_1} - \lambda_1 N_1 L, \tag{33}$$

which, upon integration, becomes

$$N_1L = \frac{rQ_L}{V\lambda_1^2}[1 - \exp(-\lambda_1 t)]. \tag{34}$$

Since the assumption is made that the $^{135}I/^{135}Xe$ pair is at radioactive equilibrium, t in Eq. 34 refers to the time after the beginning of the leak.

The ^{135}Xe tramp component in the primary system is simply

$$N_2T = \frac{Q_T}{\lambda_2}. \tag{35}$$

The formation rate of ^{135}Xe in the primary coolant for the extruded sodium bond is

$$\frac{dN_2L}{dt} = \frac{rQ_L}{V\lambda_1}[1 - \exp(-\lambda_1 t)] - \lambda_2 N_2 L. \tag{36}$$

After integration, Eq. 28 becomes

$$N_2L = \frac{rQ_L}{V\lambda_1\lambda_2(\lambda_1 - \lambda_2)}\{\lambda_1[1 - \exp(-\lambda_2 t)] - \lambda_2[1 - \exp(-\lambda_1 t)]\}. \tag{37}$$

The ^{135}Xe activities originating from tramp and leak sources are shown in Fig. 7. As in the previous examples, a leak rate of 5.5×10^{-6} cm^3/sec is assumed. Of particular significance is the behavior of the leak component. In this case the slow continuous or intermittent type of leak does not lead to a peak; rather, a new buildup curve starts when the leak develops. Eventually the ^{135}Xe activity associated with the leak reaches a new and higher equilibrium value.

The S/N ratio for the case illustrated is simply the ratio of Eq. 37 to Eq. 35; hence,

$$\text{S/N ratio} = \frac{rQ_L}{V\lambda_1(\lambda_1 - \lambda_2)\,Q_T}\{\lambda_1[1 - \exp(-\lambda_2 t)] - \lambda_2[1 - \exp(-\lambda_1 t)]\}. \quad (38)$$

At $t = \infty$, the S/N ratio reduces to

$$\text{S/N ratio} = \frac{rQ_L}{V\lambda_1 Q_T}. \quad (39)$$

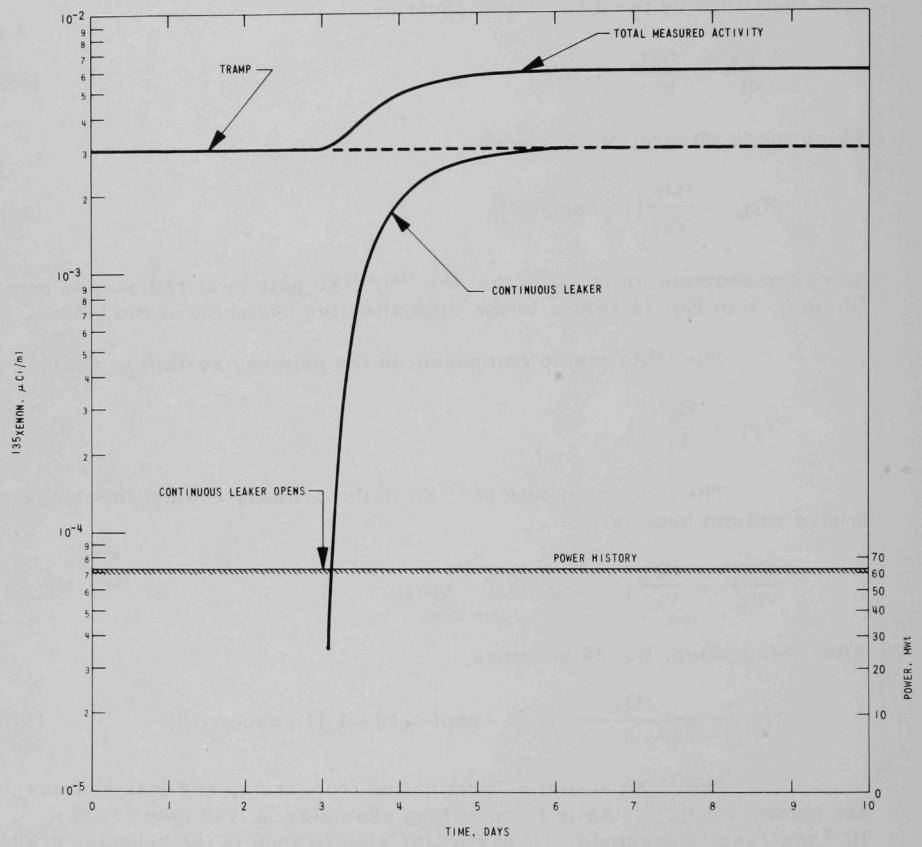

Fig. 7. Xenon-135 Activity Generated by a Slow, Continuous (or Intermittent) Release of Bond under Equilibrium Conditions

6. Case 6. Slow Loss of Bond, followed by a Reactor and Primary-pump Shutdown

In this example, the assumption is made that the ^{135}I and ^{135}Xe are in equilibrium in the fuel element and in the primary system. A slow leak

develops, and the reactor and primary coolant pumps are shut down. In practice, the coolant pumps are not shut off immediately after reactor shutdown. The assumption here of a coincident reactor and pump shutdown is made for convenience and changes the illustration only slightly.

Assuming a coincident reactor and pump shutdown at $t = 0$, where t is the time after shutdown, the ^{135}Xe in the primary system from tramp origin consists of two components: the tramp ^{135}Xe present at $t = 0$, and the ^{135}Xe generated after shutdown from the decay of tramp ^{135}I.

The first tramp component is simply

$$\left(\frac{dN_2T}{dt}\right)_1 = Q_T \exp(-\lambda_2 t). \tag{40}$$

The second tramp component is

$$\left(\frac{dN_2T}{dt}\right)_2 = \frac{Q_T\lambda_2}{\lambda_2 - \lambda_1}[\exp(-\lambda_1 t) - \exp(-\lambda_2 t)], \tag{41}$$

and the sum is

$$\left(\frac{dN_2T}{dt}\right)_{\substack{\text{total}\\ \text{tramp}}} = Q_T \exp(-\lambda_2 t) + \frac{Q_T\lambda_2}{\lambda_2 - \lambda_1}[\exp(-\lambda_1 t) - \exp(-\lambda_2 t)]. \tag{42}$$

The ^{135}I inventory in the sodium bond of the fuel element at $t = 0$ is Q_L/λ_1. Thereafter, the inventory decays according to

$$N_{\text{inventory}} = \frac{Q_L \exp(-\lambda_1 t)}{\lambda_1}. \tag{43}$$

The net rate of change of ^{135}I in the primary coolant from the leak is

$$\frac{dN_1L}{dt} = \frac{rQ_L \exp(-\lambda_1 t)}{\lambda_1 V} - \lambda_1 N_1 L, \tag{44}$$

which yields

$$N_1L = \frac{rQ_L t \exp(-\lambda_1 t)}{\lambda_1 V}. \tag{45}$$

The ^{135}Xe growth rate from the integrated form of the source term, Eq. 45, is then defined by

$$\frac{dN_2L}{dt} = \frac{rQ_L t \exp(-\lambda_1 t)}{V} - \lambda_2 N_2 L, \tag{46}$$

which, upon integration, becomes

$$N_2L = \frac{rQ_L}{V(\lambda_2 - \lambda_1)^2}\{\exp(-\lambda_2 t) + \exp(-\lambda_1 t)[(\lambda_2 - \lambda_1)\, t - 1]\}. \qquad (47)$$

The ^{135}Xe activities from tramp and leak origin are shown in Fig. 8. As in the previous cases, a leak rate of 5.5×10^{-6} cm^3/sec is assumed. Addition of the two components gives the ^{135}Xe activity that would be sensed by the fission-product monitors. Note that the ^{135}Xe originating from the leak differs from that illustrated in Case 5, the slow release of bond sodium under operating conditions. For Case 6 (see Fig. 8), the ^{135}Xe activity associated with the leak builds up to a maximum and then decays away to zero. The difference is caused, of course, by the termination of power operation in Case 6.

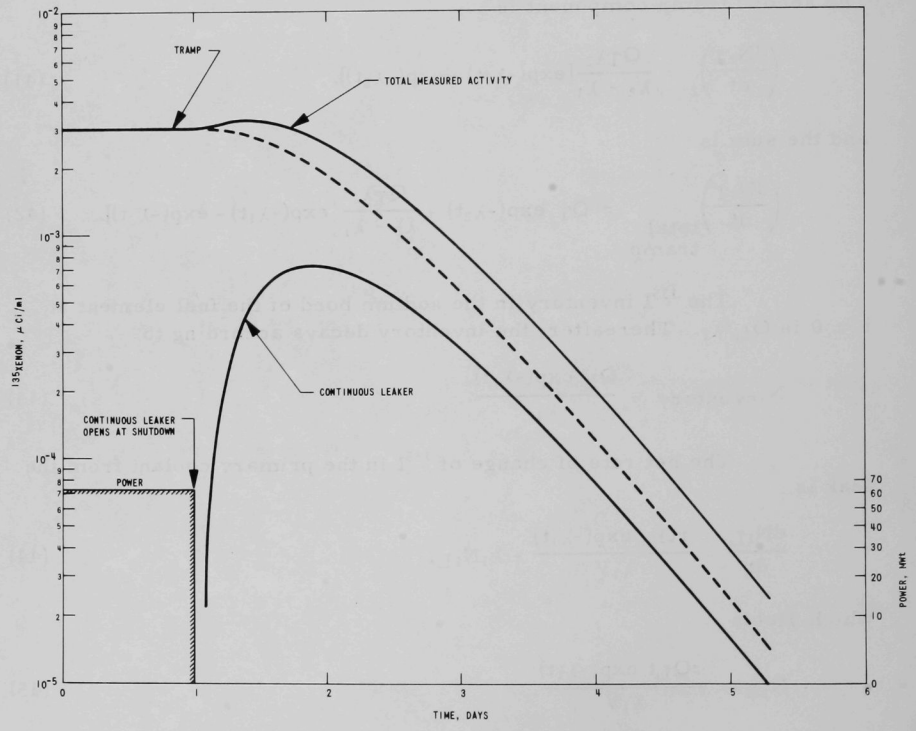

Fig. 8. Xenon-135 Activity Generated by a Slow, Continuous (or Intermittent) Release of Bond following Reactor and Pump Shutdown

7. Case 7. Rapid Loss of Bond, followed by a Reactor and Primary-pump Shutdown

Assuming that the entire annulus of the element is voided within a matter of seconds or minutes and that the reactor and pumps are shut down shortly thereafter, the ^{135}Xe activity from tramp origin is given by Eq. 42. Thus,

$$\left(\frac{dN_2T}{dt}\right)_{total} = Q_T \exp(-\lambda_2 t) + \frac{Q_T\lambda_2}{\lambda_2 - \lambda_1}[\exp(-\lambda_1 t) - \exp(-\lambda_2 t)]. \qquad (48)$$

The number of ^{135}I atoms in the bond inventory shortly before $t = 0$ is Q_L/λ_1. Thus Q_L/λ_1 atoms of ^{135}I are assumed to be released instantaneously to the primary coolant at $t = 0$. By the same logic as used in Eqs. 25-27 the buildup of ^{135}Xe from this source is described by

$$N_2L = \frac{Q_L}{\lambda_2 - \lambda_1}[\exp(-\lambda_1 t) - \exp(-\lambda_2 t)]. \qquad (49)$$

The ^{135}Xe activities associated with tramp and leak origins are illustrated in Fig. 9. Note that in this case the ^{135}Xe activity from the leak peaks sharply at $t = 11.6$ hr, whereas for Case 6 the peak was considerably delayed in time. The amount by which the peak is delayed, then, may be used to characterize the nature of the leak, i.e., whether it is slow, intermediate, or instantaneous. In fact, if simplifying assumptions are invoked, the mathematical development given above can be used to estimate the leak rate r, since the ratio Q_L/Q_T used in the various expressions is known from the exposed-fuel calibration studies.

All the foregoing considerations have been based on two tacit assumptions. One is the assumption that the rate of bond release is constant throughout the extrusion process. This, of course, is not true, since the leak rate would decrease as the plenum pressure in the element decreased. Insofar as the illustrations cited above are concerned, consideration of decrease-of-rate effects would change amplitudes but would not significantly alter the qualitative nature of the illustrations. The other assumption is based on a uniform distribution of the ^{135}I inventory in the annulus only. Again, this assumption does little to compromise the value of the illustrations.

If decreasing leak rates are considered and if the exact ^{135}I distribution in the bond is considered, the equations become quite complex. Illustrations of how refinements increase the complexity of the mathematical development have been given by Fryer *et al.*[12,13]

The illustrations given above are not intended to provide a basis for quantitative evaluation. Rather, they have been assembled to

illustrate how information derived from the various fission-product monitors can be used on an inferential basis to characterize the nature of a release involving the loss of bond sodium. There is no reason, however, why refinements cannot be incorporated in the foregoing expressions to yield information on at least a semiquantitative basis.

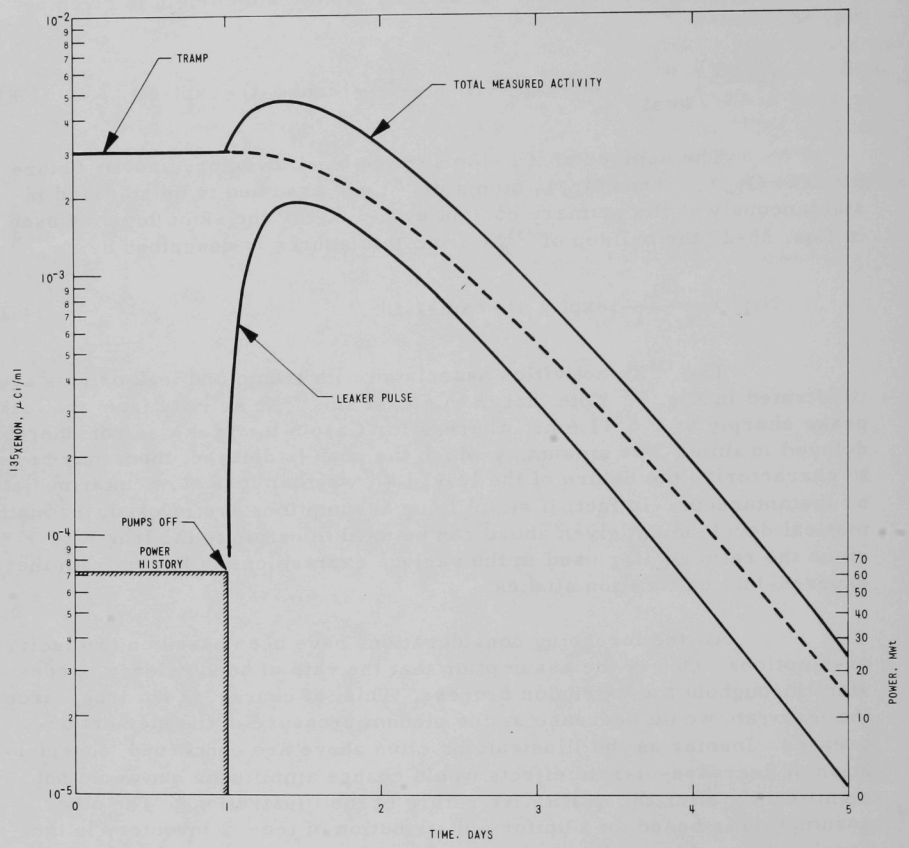

Fig. 9. Xenon-135 Activity Generated by a Pulse-type Loss of Bond following Reactor and Pump Shutdown

VII. SIMULATION OF LOSS-OF-BOND-TYPE CLADDING DEFECTS IN TREAT

As discussed in Sec. IV, the amount of sodium bond extruded through a cladding defect depends on many factors, among which are (1) the type of fuel material (low- versus high-swelling), (2) the atmospheric pressure at the place of fabrication, (3) the burnup of the fuel material, (4) the elevation of the defect with respect to the bottom of the fuel column, and (5) the position of the fuel element in the reactor. Henault[11] has evaluated the effects of each factor and concludes that the "worst case" of fuel unbonding would occur under the following conditions: (1) a low-swelling element fabricated at sea level, and (2) a burnup of 1.8 at. % in row 6, with the defect located in the vicinity of the lower weld. With these conditions and assuming a complete voiding of the annulus as bond sodium extrudes, Henault has shown that as much as 8.0 in. of fuel material could become unbonded. On the other hand, a similar fuel element located in row 1 would not unbond. Clearly, degrees of unbonding between these extremes could occur for other elements, the degree depending on fuel material, burnup, row location, and the elevation of the defect.

Precisely what happens when fuel material unbonds with the reactor operating has long been obscure. Conjecture has ranged from relatively innocuous consequences to situations in which fuel melts and "burns" through the cladding. Intuitively, the worst case appears to be one in which the entire sodium bond is voided instantaneously. Under such conditions, fuel melting is inevitable. Clearly, experimental information has been needed to define more closely the consequences and severity of unbonding phenomena.

The use of EBR-II as a facility for conducting loss-of-bond experiments was rejected, since no practical method could be found for simulating an instantaneous and complete loss of bond under normal full-power operating conditions. Attention was then directed to the use of the Transient Reactor Test Facility (TREAT)[14-17] as a facility for carrying out bond-loss simulation studies. Four experiments were conducted. Although each of these has been described elsewhere, the results are considered so important that a comprehensive review of the entire program is given here.

A. Description of TREAT

TREAT[14-17] is a versatile irradiation-test facility in which fueled samples can be subjected to sharp power transients. Because design and operational details are described elsewhere, only the features that affect an understanding of EBR-II simulation tests are discussed here.

The facility is illustrated in cutaway form in Fig. 10. The core region is approximately a right cylinder 48 in. high by 66 in. in diameter. The core is fueled with a mixture of fully enriched UO_2 dispersed in graphite. Above and below the core region are graphite reflectors, each 24 in. thick.

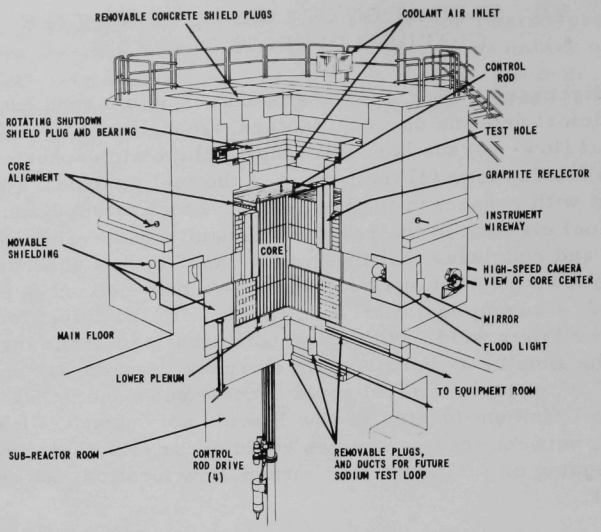

Fig. 10. Cutaway View of TREAT. ANL Neg. No. 112-771.

The large amount of graphite in the core (graphite-to-fuel ratio of about 10,000) serves two principal purposes: as a moderator, and as a heat sink during a power transient. Sharp, super-prompt-critical transients are initiated by tripping a boron-loaded transient rod from the core. During the transient, thermal energy is absorbed by the graphite. The increase in graphite temperature increases the leakage probability by hardening the neutron spectrum. Accordingly, self-limiting transients in the super-prompt-critical regime can be run. The large heat capacity of the graphite serves to protect the system from thermal damage. Transients with periods as short as 30 msec can be conducted. Integrated power bursts up to 2100 MW-sec are also possible.

Fuel samples are irradiated in vehicles that replace one or more fuel assemblies. By adjusting the fuel composition in the samples and programming the time-power behavior of the reactor, a wide range of transient conditions can be simulated in the fuel samples (usually complete fuel elements).

B. The Mark-I Flowing-sodium Loop

Transient conditions in EBR-II driver-fuel elements can be simulated in the Mark-I flowing-sodium loop,[18] a vehicle that replaces a single TREAT fuel element. The loop, illustrated in Fig. 11, consists essentially

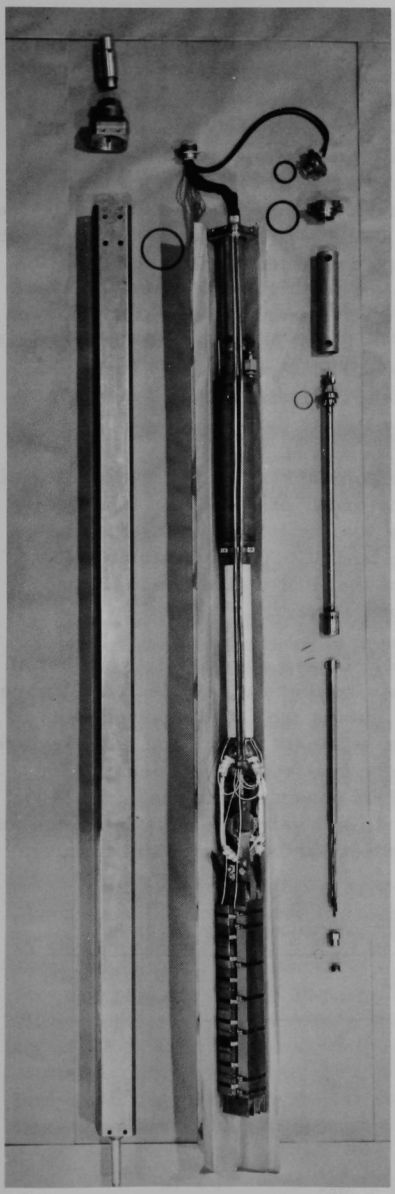

Fig. 11. Mark-I Flowing-sodium Loop for Use in TREAT (upper portion of loop at the left of the photograph). ANL Neg. No. 112-686.

of a test section supplied with flowing sodium. Sodium is pumped in a closed-loop manner through the test section by an electromagnetic pump. Power is supplied to the pump by a specially wound transformer, which is suspended inside the loop shroud slightly below the loop circuits. The loop circuits include an electromagnetic flowmeter, NaK-filled pressure transducers, thermocouples, and heaters. The heaters are used to bring the loop to operating temperature before the transient.

The test section accepts a seven-element cluster of EBR-II driver-fuel elements on a standard EBR-II pitch. The test section is inserted through the top-end plug of the loop; the lower end of the test section is seated against a seal fitting to ensure a continuous flow of sodium through the test section. Power and instrument leads are led through the top of the loop.

This type of loop has been found extremely useful as a vehicle for studying the effects of fuel unbonding under typical EBR-II conditions of power, coolant flow rate, and temperature. In all the studies discussed below, the transients were of the "flat-topped" type; i.e., TREAT power was increased rapidly to some predetermined power level, held at this power level for 6-7 sec, and then dropped rapidly through scram action. By adjusting the fuel content of the test specimens and adjusting the TREAT power level during the flat-topped portion of the transient, realistic conditions of power density, coolant flow, and temperature in the test specimens were simulated. Various conditions of bond loss were simulated when preparing the test specimens. In all, four flat-topped transients were conducted. In each of these, the test specimen was located at the center of a seven-element cluster which occupied the test section of the loop.

C. Simulation of Completely Unbonded Elements, ID-RP-1 and ID-RP-2

In these studies, the two test specimens consisted of standard Mark-IA driver elements, both of which were fabricated without sodium bond.[19-23] Argon gas at atmospheric pressure filled the annulus between the fuel pin and the cladding. Flat-topped transients were conducted on each specimen. Except for the TREAT power regime, both tests were essentially the same. In both cases, the enrichment of the test specimen was 6% (^{235}U). In the first test, ID-RP-1, the TREAT power regime was chosen to simulate the power density in a standard driver element located at the center of the EBR-II core with the system operating at the (then) nominal power rating of 50 MWt. A modest degree of conservatism was imparted to the tests by biasing the TREAT power regime. As it turned out, the test specimen operated for approximately 7 sec at a power density that corresponded to that in a standard driver element operating at core center at 57-MWt (EBR-II) conditions.

Because of the short thermal time constant of EBR-II fuel material, i.e., 0.2-0.3 sec, transient durations of the order of 7 sec are sufficiently long to achieve thermal equilibrium in the fuel material during the flat-topped portion of the transient. Thus, the test effectively simulated the behavior of an EBR-II driver-fuel element that had instantaneously and completely lost its bond under 57-MWt conditions.

The other test in this series, ID-RP-2, was essentially a repeat of ID-RP-1, except that the test specimen was deliberately subjected to more severe power and temperature conditions during the flat-topped portion of the transient. Table I, which summarizes pertinent power and temperature information for both tests, indicates that the test specimen operated for approximately 6 sec under simulated EBR-II power conditions of 90 MWt. Also summarized in Table I are initial and final values for the inlet-coolant temperature and the difference between outlet- and inlet-coolant temperatures during the transient.

TABLE I. Experimental Conditions for Tests ID-RP-1 and ID-RP-2

Parameter	ID-RP-1	ID-RP-2	EBR-II at 50 MWt, Central Pin
Flat-top duration, sec	6.9	6.2	-
Equivalent EBR-II power, MWt	57	90	50
Power density of fuel material, W/cm^3	3100	4900	2700
Coolant temperature, °F			
Inlet, initial	734	815	700
Inlet, final	806	952	-
Rise[a]	180	209	130

[a]Mixed mean sodium-temperature rise from inlet to outlet, at steady-state power during the transient.

Nondestructive and destructive examinations were conducted on the test specimens. The results of visual examinations conducted on the ID-RP-1 specimen indicated a complete absence of cladding damage. No evidence of distortion was found; the dimensions of the cladding were still consistent with fabrication specifications.

Additional visual examinations were conducted after the cladding was stripped from the fuel. Figure 12 is a photograph of the fuel material. Clearly, fuel had slumped, flowed, and cast against the colder cladding. Evidence of shiny fuel-cladding eutectic alloy was noted. Also noted was a layer of material that surrounded the fuel. Physically, it appeared as if fuel material had melted and had been constrained for a short time in a sack which subsequently broke and allowed molten material to run under the influence of gravity. Although the composition of the sack was never identified, it seems reasonable to assume that the chemical form was that of an oxide.

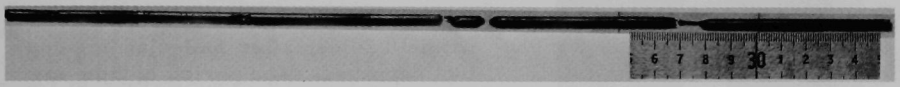

Fig. 12. Reconstructed Specimen from ID-RP-1. Notice sack-like structure that, presumably, momentarily contained molten fuel. ANL Neg. No. 112-8307.

The attack on the cladding by the hot (perhaps molten) fuel was minor. No evidence of a penetration depth greater than 0.001 cm was noted. (Nominal cladding thickness is 0.022 cm.) The results of metallographic examinations revealed that the fuel material had a relatively uniform fine-grained matrix. Grain sizes were of the order of 25 μ. Since grain sizes in production pins ranged from 25 μ at the top to approximately 100 μ at the bottom, this evidence suggested the rapid cooling of a molten alloy. Additional evidence of melting was indicated by the presence of shrinkage voids and irregular surfaces (see Fig. 12).

As described above, specimen ID-RP-2 was irradiated under more severe conditions. Even so, no external evidence of cladding damage was noted. Again, external cladding dimensions were consistent with fabrication specifications. After the cladding was stripped away, the appearance of the fuel surface resembled that of ID-RP-1, except that a greater amount of shiny-appearing fuel-cladding eutectic alloy was noted. Evidence also indicated the presence of a sack that tended to prevent contact between the molten fuel material and the cladding. Where the sack had split, permitting fuel-cladding contact, eutectic formation was evident. Such action is illustrated in Fig. 13, a photograph of matching fuel and cladding surfaces.

Slumping phenomena were greater for ID-RP-2 than for ID-RP-1. The top of the fuel column slumped approximately 2 cm; substantial voids were evident. Cladding penetration, too, was more severe. For the most aggravated case, fuel material penetrated to a depth of approximately 11% of the cladding thickness.

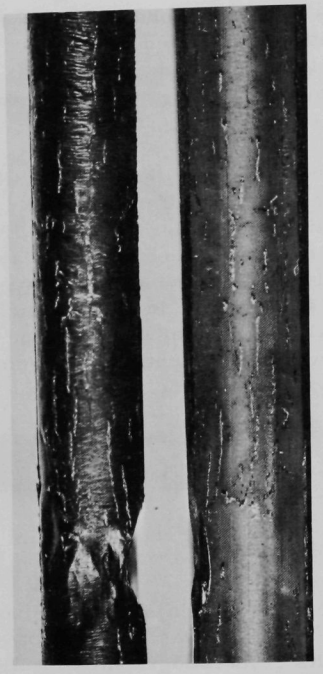

Fig. 13. Macrophoto of Fuel Surface of ID-RP-2 and Matching Inner Surface of Cladding. Neg. No. MSD-50928.

Based on an idealized meltdown model, transient heat-transfer calculations were carried out.[24] The results of the calculations indicated that the fuel surface of ID-RP-1 cooled too rapidly to permit significant penetration of the cladding by eutectic formation, even for penetration rates of approximately 0.025 cm/sec, which are considered typical for attack by molten fuel.[25,26]

The more severe transient, ID-RP-2, provided a more sensitive assessment of the model. The maximum fuel-surface temperature was calculated to be 1994°F. However, the fuel surface decreased below the fuel solidus of 1836°F within 0.20 sec after fuel-cladding contact occurred. The period of time for which the maximum value of the inner-surface cladding temperature remained above 1832°F (1000°C) was shown to be approximately 0.25 sec. Under isothermal conditions, the rate of attack of stainless steel by molten uranium-5 wt % fissium alloy just above the liquidus is about 0.025 cm/sec. Hence the cladding attack for ID-RP-2 can be predicted to be <0.005 cm; this value agrees well with the observed 0.0025 cm.[19]

D. Simulation of Partially Bonded Elements, EBR-MF-1 and EBR-MF-2

Although the results of the transient tests conducted on the two completely unbonded specimens, ID-RP-1 and ID-RP-2, were important in demonstrating melting and recasting phenomena, the fact that all surfaces were free of sodium removed a degree of realism with respect to loss-of-bond failures in the reactor. If an element should unbond while the reactor is operating, it is reasonable to believe that both fuel and cladding surfaces would remain wetted with bond sodium. Furthermore, channeling effects would be expected; i.e., the bond blowdown would not be complete and clean. Quite likely some regions of the annulus would remain bonded, whereas other portions would be swept free of sodium. In effect, the element would be partially bonded; relatively large axial and circumferential voids would be expected. To investigate the effects that such voids would have on melting and recasting phenomena, additional experiments were carried out.

1. EBR-MF-1

In the first of these experiments (EBR-MF-1), the test specimen was characterized by large longitudinal voids. A normal EBR-II Mark-IA fuel element contains enough sodium to provide an overlay 0.65 in. above the top of the fuel column. For the EBR-MF-1 specimen, the sodium inventory was reduced to an amount that would bond the pin over its lower half only. After seal welding, the element was heated, then manually tipped from the vertical to a horizontal position. During this operation, molten sodium flowed from the bottom portion of the element into the upper annulus. Care was taken to prevent the rotation of the element, since the object of the operation was to provide a bond on one side of the element and a substantial void on the other. (How well these efforts succeeded is discussed below.)

After assembly in the loop, the test specimen was irradiated under a flat-topped power regime in TREAT.[27-29] The conditions under which the irradiation was conducted are summarized in Table II. Also given is pertinent information for a standard driver element located in row 1 of EBR-II under 50-MWt operating conditions.

TABLE II. EBR-MF-1 Irradiation Conditions

	Values at Power Peak	Average for Transient	EBR-II Row 1
Reactor power, MWt	122	85	50
Pin power at axial center, W/g	420	290	150
Transient duration, sec	-	8	-
Fuel enrichment, %	-	6	52
Inlet sodium temperature, °F		(Initial 700, final 790)	700
Coolant temperature rise (mixed mean sodium-temperature rise from inlet to outlet), °F	135	-	130

Table II shows clearly that the partially bonded test specimen operated under power conditions that were significantly more severe than those associated with normal EBR-II operation.

Following the irradiation, the loop was transferred to the Fuel Cycle Facility[30] (now called the Fuels and Examination Facility) for removal and examination of the test specimen. The results of profilometry measurements demonstrated clearly the absence of cladding strain. Postirradiation

dimensions were indistinguishable from production specifications. The quality of the sodium bond and the overall conditions of the fuel material were studied by eddy-current methods. The results of these measurements indicated that, although the sodium bond was indeed deficient, the fuel material had neither melted nor slumped. The results of neutron-radiographic studies substantiated the absence of significant fuel-rearrangement effects.

The cladding was then stripped from the fuel pin by a technique involving a progressive spiral tearing of the cladding. Photographs of the fuel pin after cladding removal are given in Figs. 14 and 15. Clearly evident is a large continuous void, approximately 9 in. in length and 180 ± 50° in circumferential arc. The lower $4\frac{1}{2}$ in. of the fuel material appears to be normally bonded.

With the cladding removed, the bond arc was measured; then the fuel pin was cleaned. Following cleaning, a diameter profile was taken, hardness measurements were performed at various axial elevations, the fuel pin was sectioned and examined by optical metallographic techniques, and densities were determined at various elevations. The results of the profilometry and hardness and density measurements are summarized in Table III. Although the data clearly indicate that melting did not occur, phase changes in the fuel material seem evident. The hardness (DPH) values are low at the top of the fuel pin and tend strongly to increase toward the lower end where the sodium bond remained intact. The DPH value for uranium-fissium in the gamma (high-temperature) phase is about 180, compared to 600 for the alpha phase. The change from the alpha to gamma phase occurs over the range 1022-1229°F. Hence it seems reasonable to conclude that the lower end of the pin remained relatively cool (<1022°F), whereas material at the upper end passed through the 1022-1229°F transition region and was subsequently quenched in the gamma phase at the end of the transient.

The results of the density measurements tend strongly to confirm this conclusion, since the density of as-bonded fuel material is about 18.05 g/cm^3, whereas the density of gamma-phase uranium-fissium is about 17.75 g/cm^3.

Of particular importance is the fact that little or no change was noted in the diameter of the fuel pin. In the completely unbonded tests cited earlier, fuel material clearly flowed to the inner surface of the cladding. Such evidence indicates that despite the existence of very large voids in the bond, enough heat was removed through the remaining bonded portions to hold the fuel temperature below the melting point.

The microstructure of the irradiated fuel pin is shown in Figs. 16-18. The microstructure varies widely from the bottom of the fuel pin to the top. At the bottom (Fig. 16), the structure appears similar

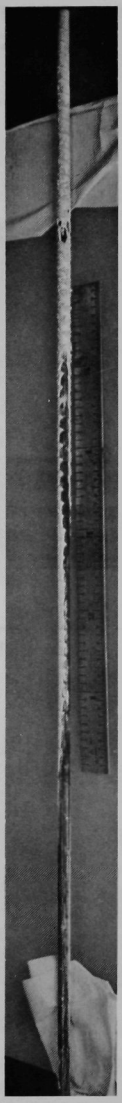

Fig. 14. Test Specimen from ID-MF-1 with Cladding Removed after Irradiation. ANL Neg. No. 103-L5646.

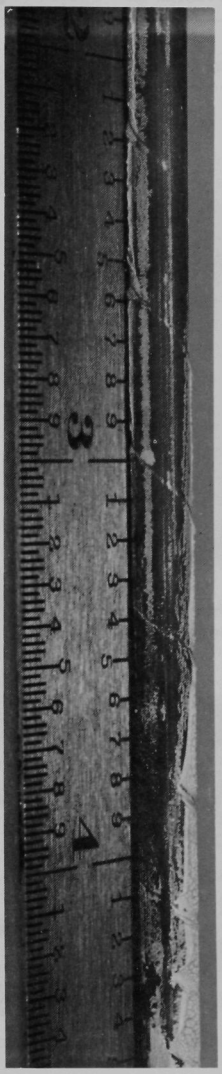

Fig. 15. Closeup View of Test Specimen from ID-MF-1 with Cladding Removed after Irradiation. ANL Neg. No. 103-L5644.

TABLE III. Postirradiation Properties of the EBR-MF-1 Fuel Pin

Position,[a] in.	Preirradiation Diameter, in.	Postirradiation Diameter, in.	Postirradiation Hardness, DPH	Postirradiation Density, g/cm^3
1	0.1436 (avg)	0.1425	-	18.05
2		0.1424	-	18.05
3		0.1435	440	18.05
4		0.1423	-	18.03
5		0.1433	-	18.04
6		0.1433	-	
7		0.1437	-	
8		0.1433	-	17.95
9		0.1436	351	17.93
10		0.1431	-	17.93
11		0.1442	-	17.94
12		0.1442	289	17.94
	Preirradiation	Postirradiation		
Length, in.	13.544	13.531		
Mass, g	64.506	64.507		

[a]Measurements were made at the distance listed from the bottom of the fuel pin.

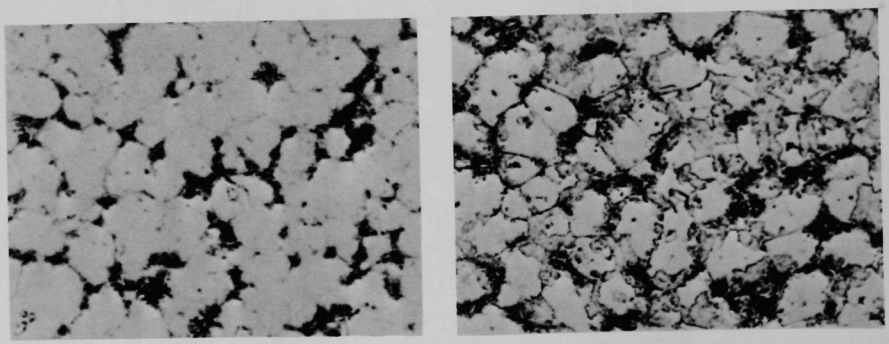

Microstructure at bottom of pin

Section taken 3 in. from bottom

Fig. 16. Microstructures at Bottom and 3 in. above Bottom of EBR-MF-1 Specimen after Irradiation. Mag. 375X. Neg. Nos. MSD-149B1-1 and -149B2-1.

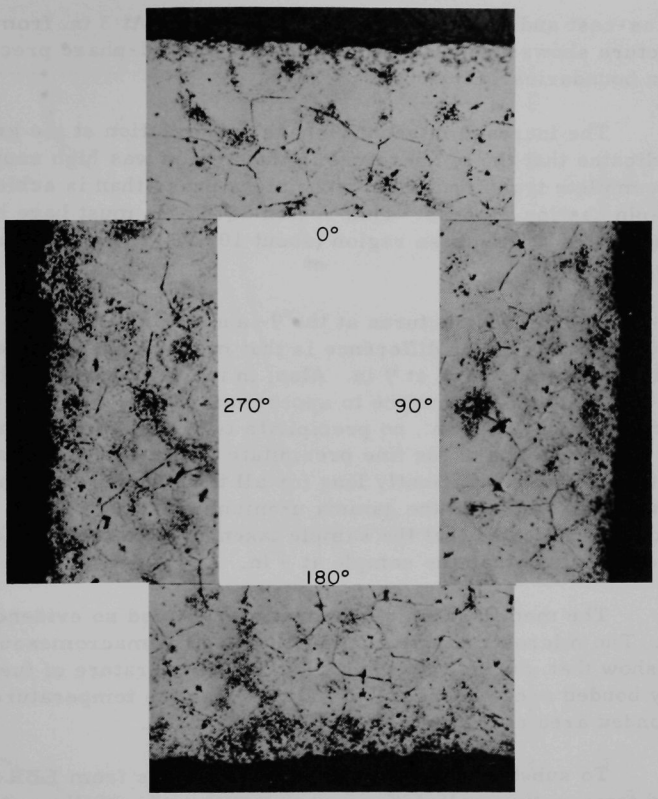

Fig. 17. Microstructures around Periphery 9 in. above Bottom of EBR-MF-1 Specimen after Irradiation. Mag. 400X. Neg. Nos. MSD-149B3-1, -2, -3, and -4.

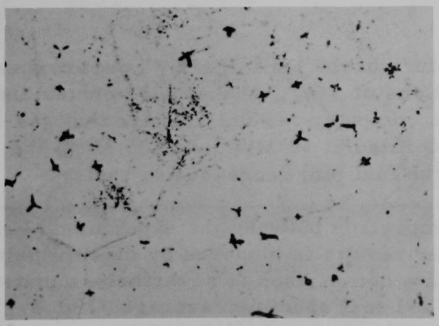

Fig. 18

Microstructure 12 in. above Bottom of EBR-MF-1 Specimen after Irradiation. Mag. 375X. Neg. No. MSD-149B4-1.

to most as-cast and many as-bonded specimens.[31] At 3 in. from the bottom, the structure shows a significant increase in second-phase precipitation at the grain boundaries.

The increase in second-phase precipitation at the grain boundaries indicates that the temperature in this region was high enough to cause a more complete transformation to the alpha phase than is achieved during the fuel-pin casting process. This region of the pin must have been heated to just below the third-phase region (about 1022°F) to achieve this transformation.

The microstructures at the 9- and 12-in. elevations are similar to each other. The major difference is that more of the fine precipitate is visible in the sample taken at 9 in. Also, in the 9-in. sample, the precipitate extends inward from the surface to approximately one-half radius, while in the specimen taken at 12 in., no precipitate is visible after about one-third radius. The existence of the fine precipitate indicates that the alloy had not been at temperature sufficiently long for all the alloying elements to be placed in solid solution in the gamma uranium produced in this region. The structure indicates that the sample taken at 12 in. reached a slightly higher temperature than the sample at 9 in.

The metallographic examination revealed no evidence of fuel melting. The microstructural examination and the macromeasurements clearly show that, during the irradiation, the temperature of fuel in the partially bonded area exceeded 1229°F, whereas the temperature of fuel in the bonded area at the bottom approached 1022°F.

To substantiate the experimental results from EBR-MF-1, idealized temperature calculations were performed with the generalized heat-transfer code THTB.[32] In this study, fuel and cladding temperatures were determined for various degrees of gas bonding at steady-state power levels in EBR-II. Families of curves giving the maximum fuel-surface and cladding temperatures as functions of power level and unbonded arc are given in Figs. 19 and 20.

The melting temperature of the EBR-II alloy is approximately 1850°F. Under the EBR-II conditions of 3 W/g-MW at core center and a coolant temperature of 900°F, the computer results indicate that gas-bond arcs as large as 260° could be tolerated at 50 MWt. At 100 MWt, the allowable gas arc (full length of the fuel pin) decreases to 150°.

Although an exact comparison between the experimental results from EBR-MF-1 and the computer results is hindered by dissimilarities in axial power shapes, an approximate comparison is nevertheless instructive. The power density in the EBR-MF-1 test specimen averaged 290 W/g, a value equivalent to that experienced by fuel material at the center of the

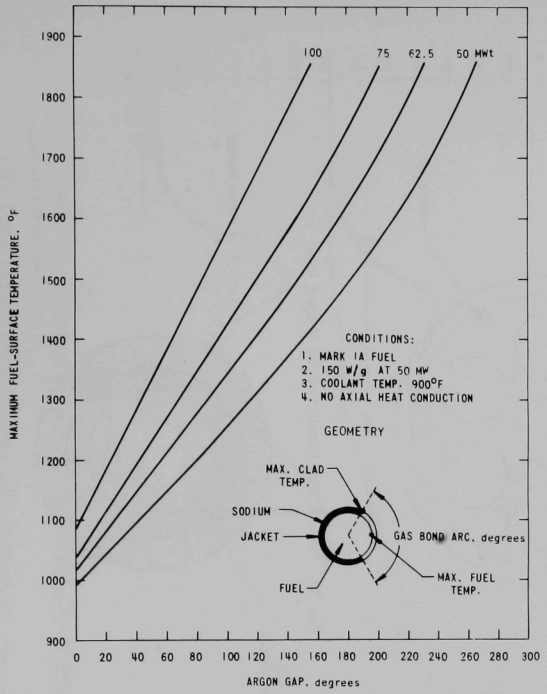

Fig. 19. Maximum Fuel-surface Temperature as a Function of Unbonded Arc in EBR-II (THTB calculation)

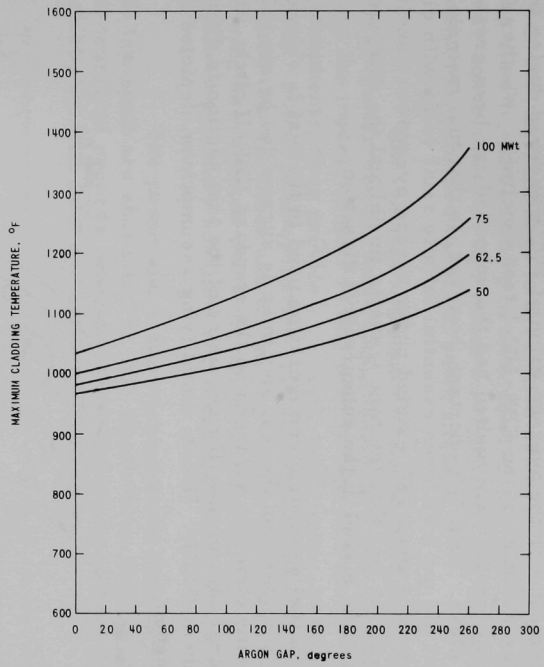

Fig. 20. Maximum Cladding Temperature as a Function of Unbonded Arc in EBR-II (THTB calculation)

EBR-II core while operating at a hypothetical power level of 97 MWt. At 97 MWt, the computer results indicate an allowable arc of 160°, a value in reasonable agreement with the average value of 180° measured during the postirradiation examination of the EBR-MF-1 test specimen. Whether fuel in the test specimen would have melted had the unbonded arc been greater than 180° is not clear. What is important, however, is that fuel material in the test specimen did not melt when essential infinite axial voids with circumferential widths of about 180° existed under severe overpower conditions. Reassuring also is the fact that the heat-transfer model and the computer program appear to be biased in the conservative direction.

The actual geometric configuration used in the test is shown in Fig. 21. In this configuration the test specimen is surrounded by six hollow argon-filled dummy elements arranged on the standard EBR-II pitch. Because of peripheral components, the geometry of the test section is difficult to describe mathematically. Hence, simplifying assumptions, depicted in Fig. 22, were needed.

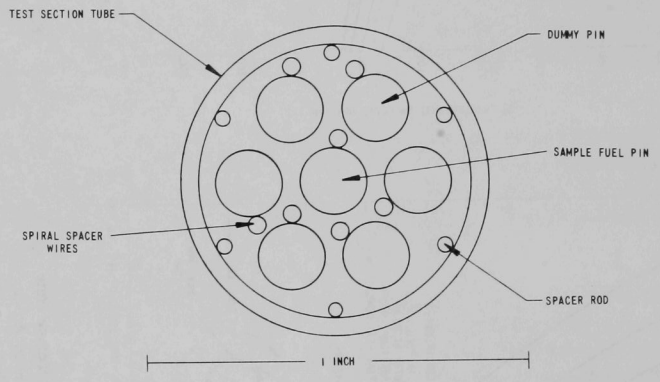

Fig. 21. Plan of Test Section of the Mark-I Loop

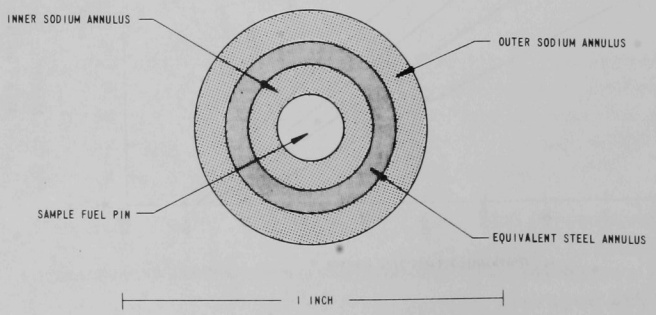

Fig. 22. Idealized Geometry Assumed for the Test Section in the THTB Calculations

Assumed was an equivalent radial geometry in which the test specimen was located at the center of the cluster and in which the total inner sodium-flow area to the center of the surrounding dummy elements was distributed according to an equivalent annulus. The dummy elements were converted to an equivalent steel annulus, and the balance of the total sodium flow formed the final, outer annulus.

The thermal resistance of the hollow dummy elements in the actual cluster was partially compensated by cross-channel mixing effects. Thus the model, similar to that used to describe the ID-RP-1 and ID-RP-2 experiments, does provide a realistic description of temperature considerations. Since the temperature calculations depend mainly on the centrally located test specimen and the sodium flow in the inner channels, the simplifying assumptions made for more outlying regions have little effect. The idealized geometry assumed in the calculations is shown in Fig. 22.

The power and sodium-temperature time dependencies during the transient are shown in Fig. 23. Power-time data were derived from the transient records, whereas the sodium-temperature data were those established with inlet and outlet thermocouples.

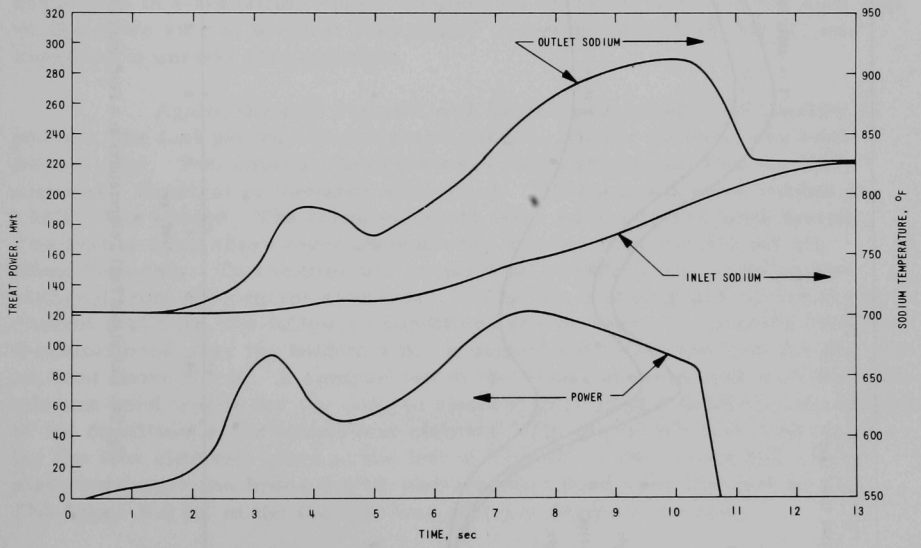

Fig. 23. TREAT Power Schedule and Inlet and Outlet Sodium Temperatures for EBR-MF-1

The fuel-temperature time dependencies during the transient are shown in Fig. 24 for three different fuel elevations. A model depicting the degree of bonding is given in the right-hand margin. Also given in the figure,

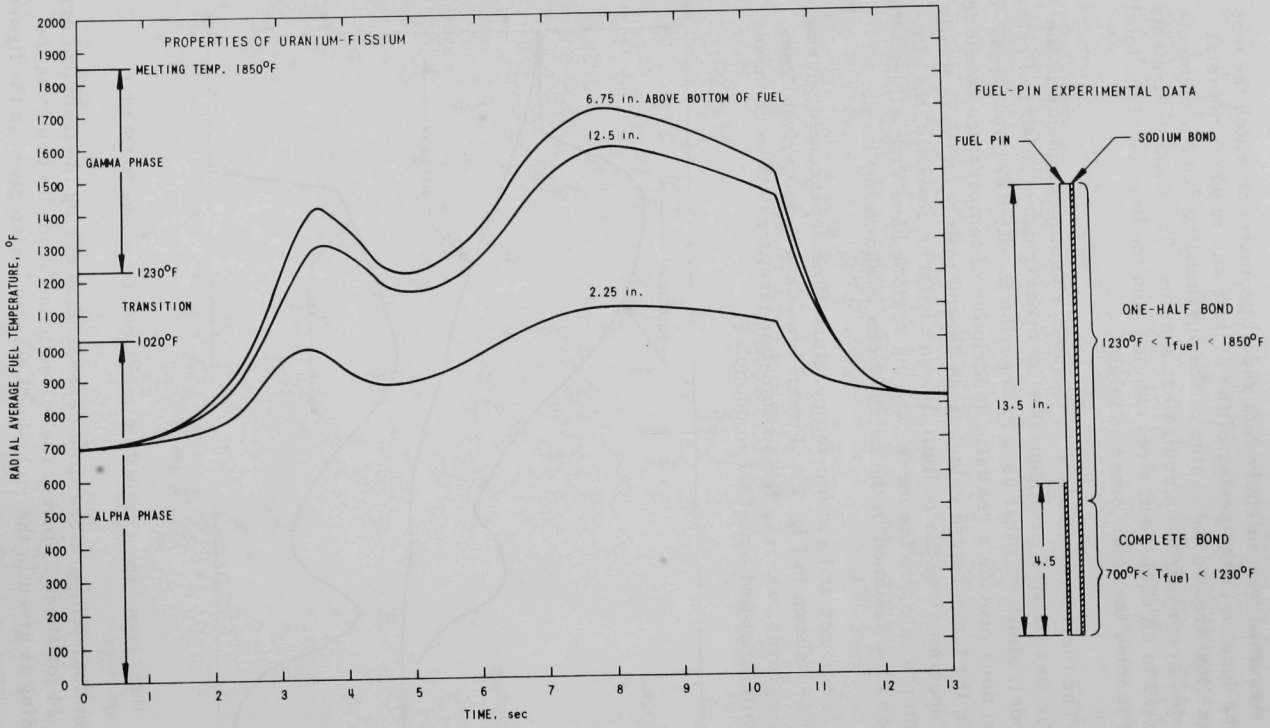

Fig. 24. Calculated Fuel Temperatures as a Function of Elevation for EBR-MF-1 Test Specimen

on the left-hand side, is a scale showing the phase regions of the fuel. Note that, whereas fuel in the lower elevations remained relatively cool and predominantly in the alpha phase, that at the upper elevation passed substantially into the gamma phase.

The results obtained from the EBR-MF-1 test are considered highly significant. The fact that large bond voids can be safely tolerated was clearly demonstrated in the test and verified by simplified but conservative physical models. Also important is the inference that the existing stringent specifications on void size could very likely be relaxed. Adding additional weight to this possibility is the fact that fuel material, over much of its productive life, is in contact with the cladding wall. Thus, the presence of a sodium bond seems important only during the beginning of fuel life.

2. EBR-MF-2

Although the results of the EBR-MF-1 tests demonstrated that the existence of partial circumferential bonds can effectively prevent fuel melting, one important question remained unanswered: What are the consequences in a transition region on one side of which fuel does not melt and on the other side of which it does melt? A second test, EBR-MF-2, was designed to answer this question.

Again, the test element was loaded with a deficient quantity of sodium, the fuel pin was inserted and settled, and the element was seal-welded shut. Two control elements were fabricated along with the test element. Identical procedures were used. The elements were bonded at 932°F, then cooled. The three elements were eddy-current bond-tested. The traces from these tests showed very similar bond quality for all three elements. To examine the actual bond condition, the cladding was stripped from the control elements. In Fig. 25, a photograph of one of the control fuel pins, the following conditions can be seen: a complete circumferential bond over the bottom 4 in., a partial bond over the next 2.5 in., and no bond above 6.5 in. A comparison of the visual observations with the eddy-current bond traces for the control element permitted a definitive evaluation of the condition in the actual test element. The preirradiation bond trace for the test element, given at the left of Fig. 26, shows that it had a complete bond over the lower 3.6 in. and a partial bond over the next 4.1 in. The upper 5.8 in. of the fuel pin was entirely devoid of sodium.

The test specimen was loaded into a Mark-I loop, which was then subjected to a flat-topped transient in TREAT. Pertinent power and temperature information are summarized in Table IV. In this case, the power regime of TREAT was deliberately chosen to provide a substantial overpower condition in the test specimen (relative to that experienced by Mark-IA fuel material located at the center of the EBR-II core under 50-MWt operating conditions). The plateau portion of the transient was

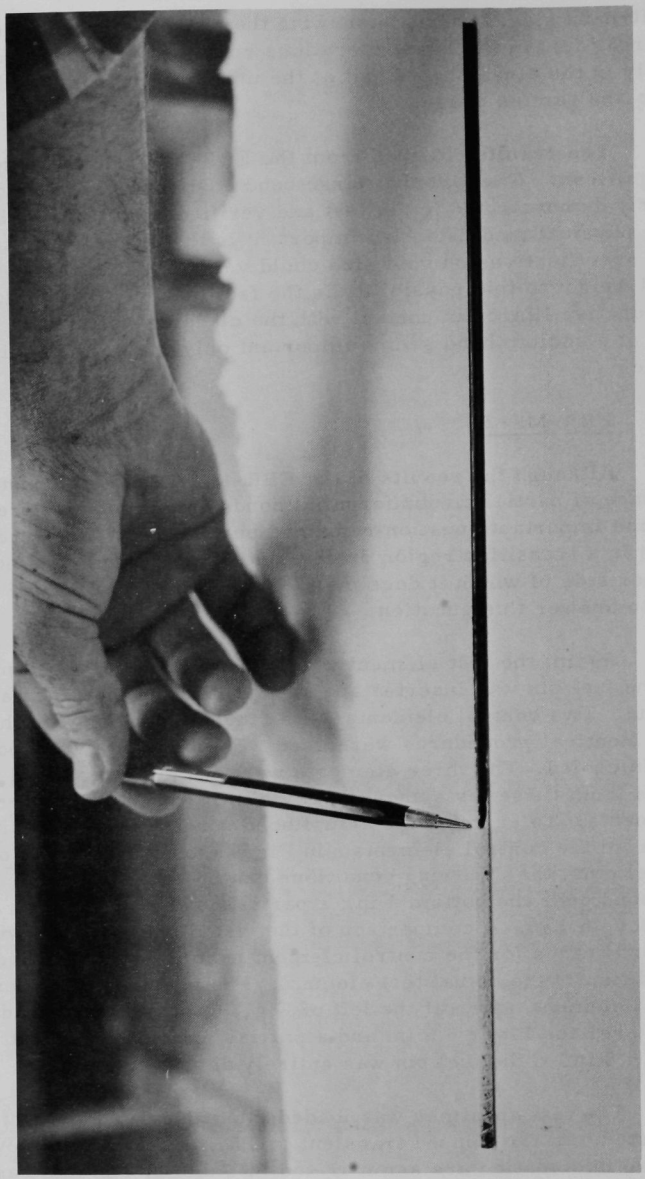

Fig. 25. Control Specimen in EBR-MF-2 Tests; Cladding Removal Revealed Complete Circumferential Voiding above 6.5 in. ANL Neg. No. 103-L5710.

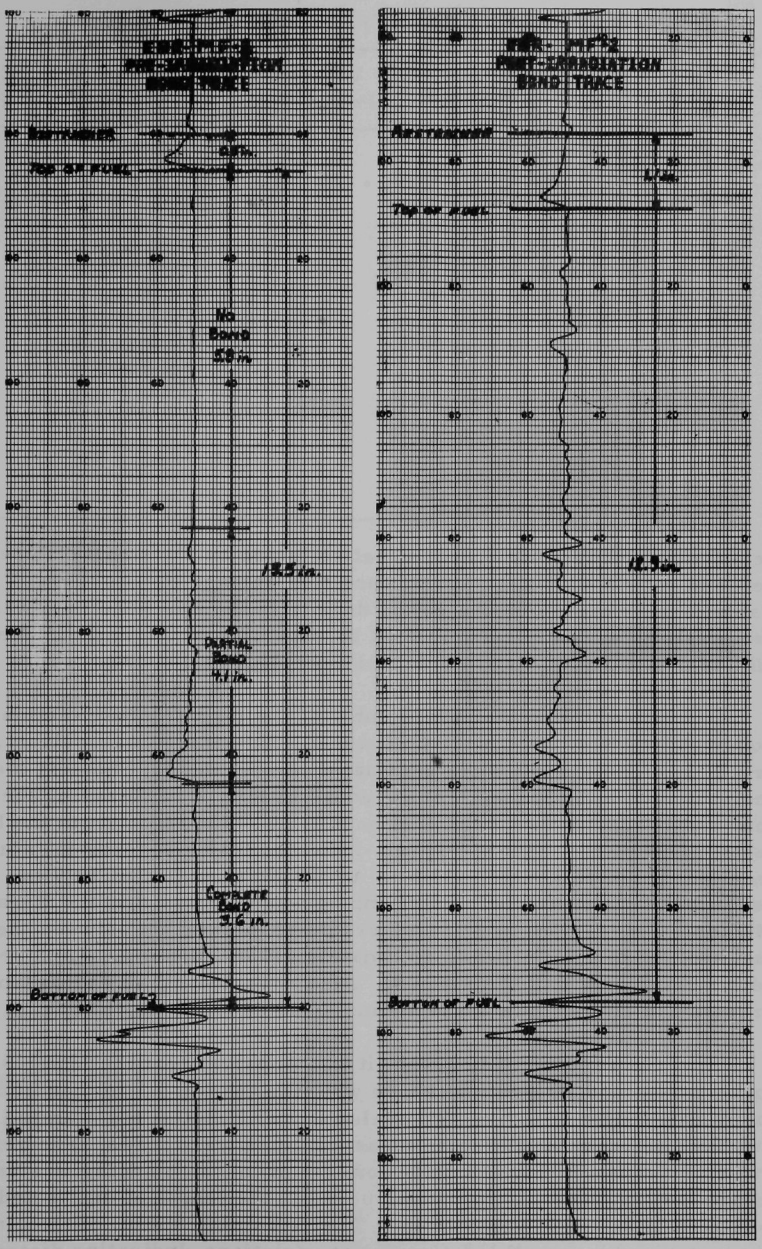

Fig. 26. Eddy-current Bond Tests on EBR-MF-2 before and after Irradiation

TABLE IV. EBR-MF-2 Irradiation Conditions

	Values at Power Peak	Average for Transient	EBR-II Row 1
Reactor power, MWt	95	88	50
Pin power at axial center, W/g	329	308	150
Transient duration, sec	-	8	-
Fuel enrichment, %	-	6	52
Inlet sodium temperature, °F		(Initial 720, final 805)	700
Coolant temperature rise (mixed mean sodium-temperature rise from inlet to outlet), °F	111	-	130

relatively flat for about 4 sec, a fact reflected by the small difference between peak and average power densities during the transient. From Table IV it is clear that the power density in the fuel specimen was approximately twice that which would be experienced by Mark-IA fuel material at the center of the EBR-II core operating at 50 MWt.

Following the disassembly of the loop, the test section was removed, washed, and visually examined. No damage was evident. Figure 27 is a photograph of the irradiated test element. The next steps in the postirradiation inspection procedure consisted of X-raying the specimen and conducting eddy-current bond tests. The trace from the bond tests, given at the right of Fig. 26, indicates that fuel material slumped from an initial elevation of 13.5 in. to a final elevation of 12.9 in. The occurrence of substantial fuel slumping was confirmed in the X-radiographic studies. Whereas the normal, unirradiated separation between the top of the fuel and the restrainer is approximately 0.4 in., the radiograph revealed a separation of 1.1 in. (see Fig. 28). Also revealed in the radiograph was the presence of large voids in the sodium bond at lower elevations.

From the radiograph, it was apparent that the lower 6 in. of the fuel pin retained its original shape whereas the top 7.5 in. had slumped to an overall length of 6.9 in. To evaluate the effects of the slumped fuel on the cladding, careful diameter measurements were made. The results of these are shown in Fig. 29. The lower 6 in. of the cladding was undisturbed. (Since the length of the spade was 0.75 in., the length of unaffected cladding was actually 6 - 0.75, or 5.25 in.) The remaining 8.2 in. of the cladding was characterized by small but significant variations, indicating distortion effects of a random nature.

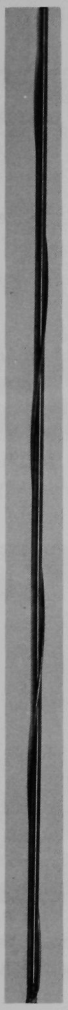

Fig. 27. Photograph of Test Specimen from EBR-MF-2 after Irradiation. ANL Neg. No. 103-M5163.

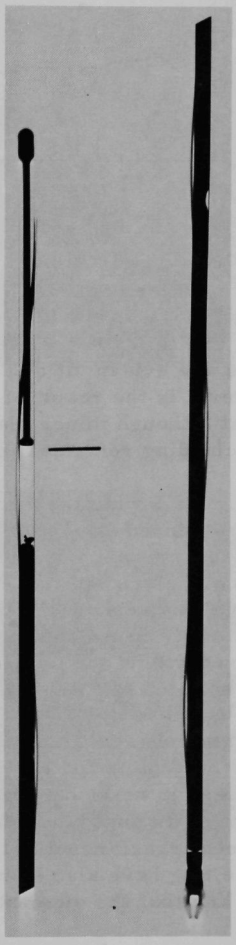

Fig. 28. X-radiograph of Test Specimen from EBR-MF-2 after Irradiation

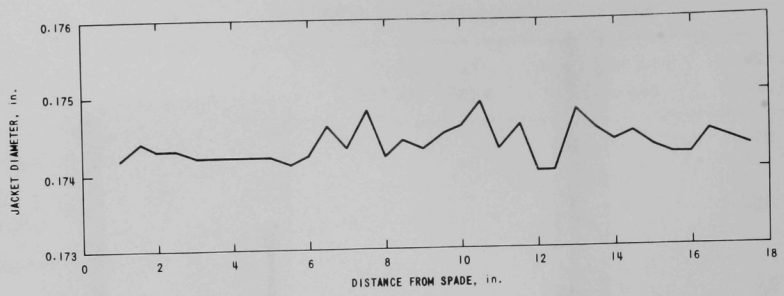

Fig. 29. Profilometry Measurements of EBR-MF-2

Major voids in the sodium bond were indicated by the radiographs at 7.9, 11.3, and 12.5 in. above the spade. The profilometry measurements in Fig. 29 correlate well with these observations, since cladding variations are evident at 8.0, 11.0, and 12.4 in. (The small peak at the 16.5-in. level is the result of the spacer-wire weld.) These results demonstrate that although minor cladding strain (approximately 0.5 mil) did result, the cladding remained intact.

Following the completion of nondestructive tests, the test specimen was sectioned for optical metallographic and hardness measurements. Macrophotos and micrographs taken at 2.5 and 5 in. from the bottom of the specimen are given in Fig. 30. An inspection of the macrophotos reveals that the fuel material retained a nearly circular shape. The microstructure of the bottom (2.5-in.) sample is typical for an as-cast fuel pin and has not been altered during the test. The microstructure of the sample taken 5 in. from the bottom indicates that some of the second-phase material (U_2Ru) has gone back into solid solution and that the uranium has all been converted to the gamma phase. These results from the microstructure correlate well with the results for the microhardness of the samples given in Table V. The decrease in microhardness exhibited by the sample taken 5 in. from the bottom of the fuel pin is further evidence that this section of the fuel pin has been transformed to the gamma phase. All the samples that exhibited melting have also been retained in the gamma phase by the relatively rapid cooling that the element experienced after the TREAT transient.

Figure 31 shows a macrophoto of the cross section of the fuel element 6.5 in. from the bottom and a micrograph of the fuel at the same elevation. The macrophoto indicates that fuel slumping has occurred in this region. The cross section of the fuel pin is no longer circular, and the width of the annulus has been reduced over three-fourths of the circumference. The microstructure of the fuel pin indicates that incipient melting has occurred. The alloy has been molten at the grain boundaries, but the entire grains have not become liquid.

192B2-3 14X

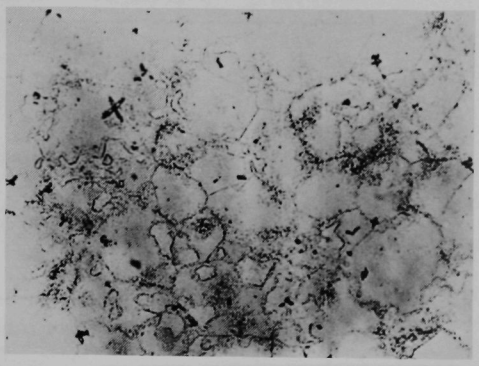

192B2-1 450X

5 in. from the bottom of the fuel pin

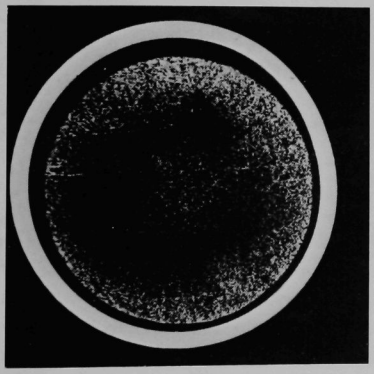

192B1-2 14X

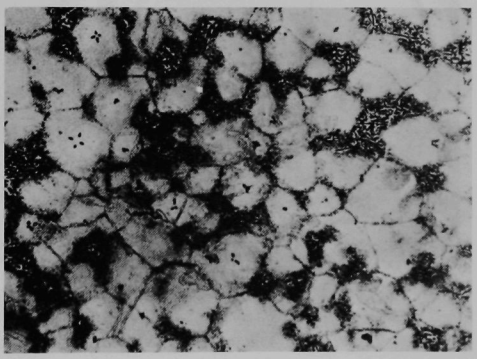

192B1-1 450X

2.5 in. from the bottom of the fuel pin

Fig. 30. Macrophotos and Micrographs of Sections of EBR-MF-2, 2.5 and 5 in. from Bottom

TABLE V. Microhardness of Samples from EBR-MF-2

Sample	Distance from Bottom, in.	Microhardness,[a] DPH, 500-g Load
192B1	2.5	463
192B2	5	233
192B3	6.5	241
192B4	9	244
192B5	Top	238
Hardness Reference Data		
	As-cast fuel	~315
	As-bonded fuel	~600
	Quenched from 1229°F (gamma)	180

[a]Average values from five measurements.

192B3-4 13.5X

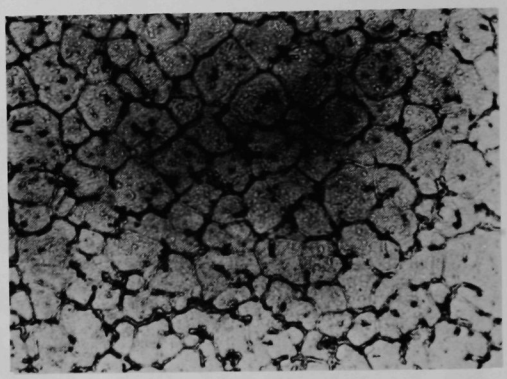

192B3-2 425X

Fig. 31. Macrophoto and Micrograph of Section of EBR-MF-2, 6.5 in. from Bottom

Figure 32 shows the macrophoto and micrograph of a section 9 in. from the bottom of the fuel pin. The macrophoto shows that the fuel pin has slumped to the extent that the fuel occupies nearly the entire ID of the cladding. Only a very thin annulus remains. Again the microstructure near the centerline indicates that incipient melting has occurred. In this sample there was also a small area where an interaction between the fuel and the cladding had occurred. The microstructure in this area indicates that sufficient liquid fuel was in contact with the cladding to dissolve part of the cladding and form liquid eutectic alloy. There is no evidence of diffusion of the fuel into the cladding, thus indicating that the interaction occurred in a liquid state. A slight reduction in the wall thickness of the cladding occurred in this area.

192B4-3 14X

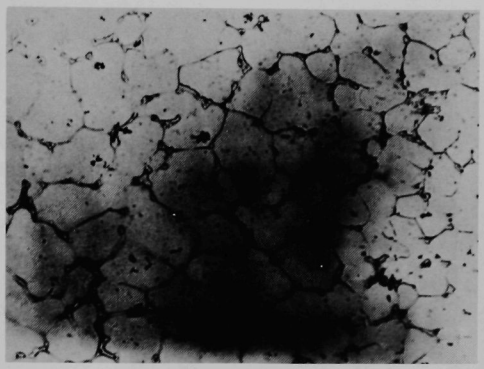

192B4-1 450X

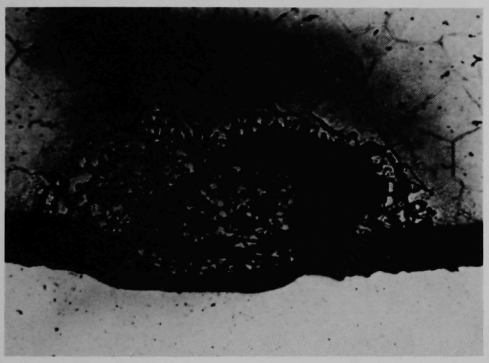

192B4-2 450X

Fig. 32

Macrophoto and Micrographs of Section of EBR-MF-2, 9.0 in. from Bottom

Figure 33 shows a macrophoto of a longitudinal section of the very top of the fuel pin and micrographs of selected areas of the pin. The macrophoto shows that the fuel slumped to a considerable extent at the top of the fuel pin. The disconnected portion of the pin (small piece above the top of the pin) may have been prevented from slumping by a string of oxide inclusions that runs through it. The microstructure at the top of the pin shows melting at the grain boundaries, but the entire grains do not appear to have become liquid. There was also an area in this sample where fuel-cladding interaction occurred. The microstructure in this area indicates that the molten fuel reacted with the cladding, dissolving part of the cladding to form the eutectic composition. Melting of the fuel-stainless steel alloy extending into the fuel to a depth of about 0.004 in. is evident in this longitudinal section. The wall thickness of the cladding was reduced by 0.001-0.002 in. in this region.

192B5-4 14X

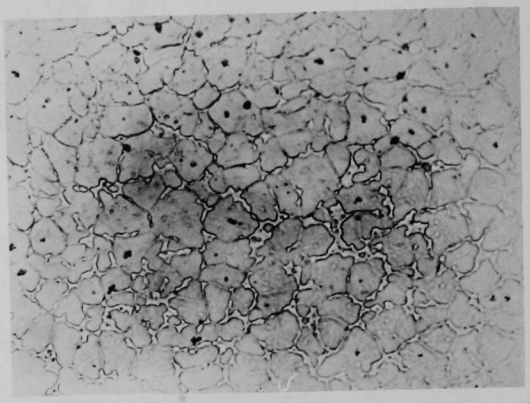

192B5-3 450X

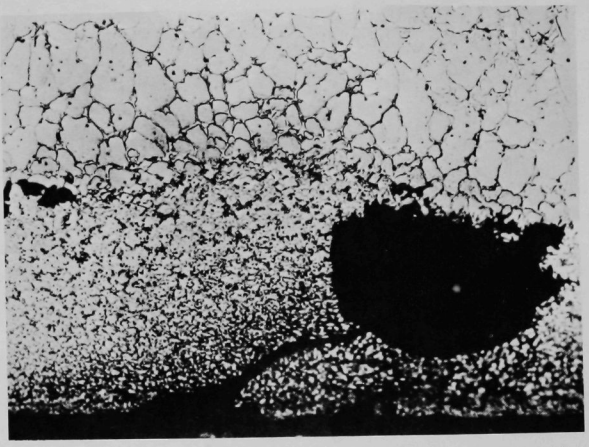

192B5-2 450X

Fig. 33

Macrophoto and Micrographs of Longitudinal Section at Top of EBR-MF-2

The hardness data in Table V correlate well with the optical examination. Near the bottom of the pin, the hardness falls between as-cast and as-bonded data. The values observed at 5, 6.5, and 9 in. and the top of the pin approach the value for nearly pure gamma-phase alloy.

The power and the sodium-temperature time dependencies are shown in Fig. 34. As mentioned above, the shape of the transient was characterized by a relatively constant power-generation rate for approximately 4 sec. The results of the postirradiation examinations were clearly consistent with those expected from an element completely bonded at the bottom, partially bonded in the middle, and completely unbonded at the top.

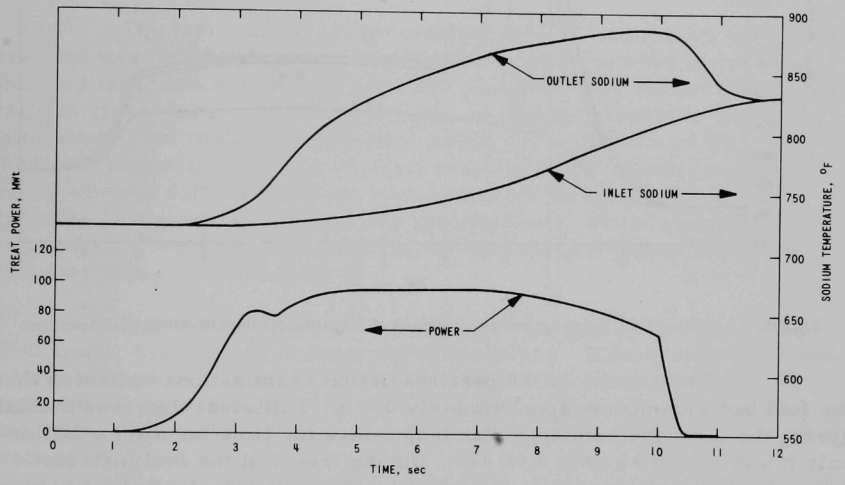

Fig. 34. TREAT Power Schedule and Inlet and Outlet Sodium Temperatures for EBR-MF-2

As a further check on this interpretation of the results, a series of heat-transfer calculations was carried out. The geometry used in the EBR-MF-1 calculations was assumed, but the problem had to be divided into two parts. The first part of the program described fuel temperatures up to the point of fuel slumping. The second part of the program considered the revised fuel geometry due to slumping. Figure 35 shows the computed fuel temperature versus time at various elevations.

At the 9.2- and 12-in. elevations, the computer code predicts fuel melting early in the transient. Melting, of course, begins at the center of the fuel pin and proceeds radially outward. When the outer fuel surface melts, slumping begins.

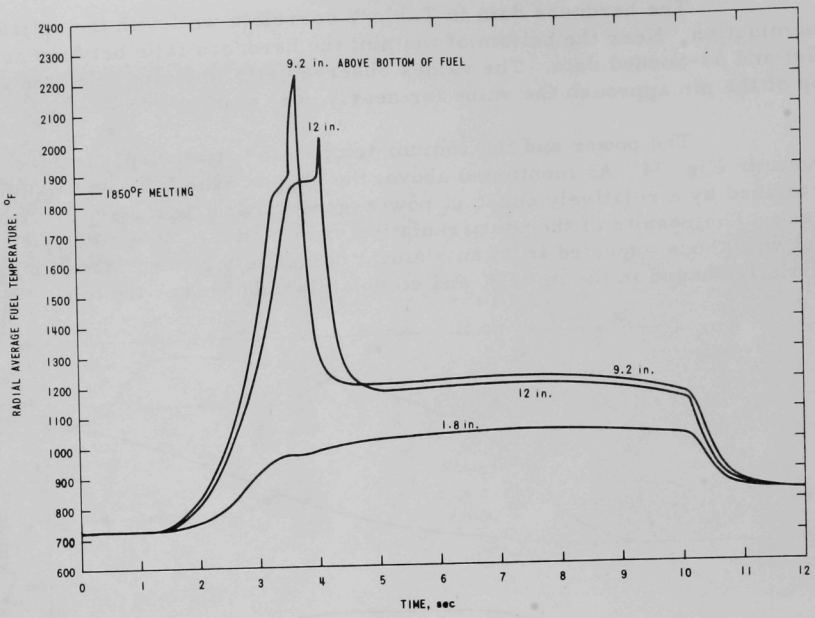

Fig. 35. Calculated Fuel Temperatures as a Function of Elevation for the EBR-MF-2 Fuel Specimen

The results of the postirradiation examinations indicated that the fuel had slumped by approximately 0.6 in. Sufficient time was available during the tests for complete slumping, since the time for a free-fall of only 0.6 in. would be only 0.06 sec. During free-fall the fuel material "superheats"; i.e., energy is absorbed by the molten fuel. Quite likely, the actual fuel motion before cladding contact would be better described as viscous flow. Hence, the free-fall value of 0.06 sec should be regarded as a lower limit.

The assumption of a free-fall time of 0.06 sec is reflected in the computed results in Fig. 35. Clearly, the amplitude of the superheat spike is sensitive to the fall time before cladding contact. Hence, the behavior illustrated should be considered as a qualitative rather than quantitative result.

At the time when fuel contacts the cladding, the computer code considers quenching action. The temperature computation at the 9.2-in. level indicates that the fuel-cladding interface temperature exceeded 1850°F for approximately 0.1 sec. Assuming a cladding penetration rate of 11 mils/sec from the data of Walter et al.,[25,26] a penetration of approximately 0.001 in. can be estimated. Such a value is in reasonable agreement with the observed penetration value of 0.001-0.002 in.

The results of the EBR-MF-2 test clearly demonstrate that the bottom of the pin, which was bonded, experienced normal irradiation temperatures for the power conditions. At the 5-in. level, in the partially bonded area, the fuel did not slump or deform, but was converted to the gamma phase, thus indicating that it experienced a temperature of 1229°F or greater. From the 6.5-in. level upward, melting occurred (approximately 1850°F) at the grain boundaries with attendant fuel slumping. Some fuel-cladding interactions occurred above the 6-in. level. The maximum observed cladding reduction was 0.002 in., or 22% of the wall thickness. The interaction of fuel and cladding produced jacket strains up to 0.0005 in., or 0.3% of the average cladding diameter (0.165 in.).

The fact that the jacket retained 80% or more of its wall thickness, and was only slightly strained, indicates that over the short term, continued irradiation would not pose any problem. The recast fuel is generally in close contact with the cladding, so that heat transfer would be maintained. The coolant flow channel would not be influenced by the 0.0005-in. jacket strain. The nominal preirradiation jacket-diameter specification is 0.174 ± 0.001 in., and the entire jacket profile of the EBR-MF-2 element falls within this specification. These conclusions are especially encouraging in light of the fact that the power level was twice that experienced in EBR-II.

Continued, long-term irradiation of a specimen such as EBR-MF-2 could, however, pose unanswered questions. If irradiation proceeded, fuel swelling would occur. This swelling would have to be accommodated longitudinally or radially, or by a combination of both. Radial swelling would strain the jacket, and current fuel specifications limit the jacket strain to 2%.

Perhaps even more significant, further fuel-jacket interaction might occur. The mechanism involves the diffusion of uranium into the cladding, thus resulting in uranium-iron eutectic formation. This process might accelerate cladding deterioration. Clearly, such questions could best be answered with properly designed irradiation experiments in EBR-II.

VIII. INADVERTENT ACTIVITY RELEASES TO THE PRIMARY SYSTEM (ARP's) IN EBR-II

As of January 1, 1972, at least eight and possibly as many as ten cladding faults have been experienced during the normal operation of the reactor. Of these, two were identified with encapsulated experimental fuel elements, three with driver-fuel elements, three with unencapsulated mixed-oxide elements, and two, although never identified, almost certainly originated from driver elements. With only one exception, that of Subassembly X085, each of the eight identified cladding faults resulted in multiple fission-product releases; i.e., each defective capsule or element, during its residence in the core, resulted in two or more ARP's.

Because details relating to the eight identified cladding faults have been documented elsewhere, the discussion below is limited to a brief review of the circumstances involved, signal strength, monitor response, and the diagnostics used to locate and identify the leaker. For convenience, the various cladding faults will be treated chronologically. Only the first four verified cladding faults are discussed. Those occurring during 1971 are still being studied and will be reported later.

A. ARP from X011: May 24, 1967

The first verified ARP in EBR-II occurred on May 24, 1967.[33-37] Before this time, about 30,000 driver elements and about 200 encapsulated experimental fuel elements had been irradiated without any detectable release of fission products to the primary system. The first indication of fission-product activity was provided by the FGM, which alarmed at 1210 on May 24, 1967. Within minutes the readings went off scale. The reactor was shut down and attempts were made to bring the FGM readings back on scale through changes in scale settings. Such efforts were futile, and not until the gain of the amplifier was changed were the readings brought on scale. Approximately 40 min of FGM readings were lost, but estimates, based on a reconstruction of the FGM strip-chart records, indicated a S/N ratio of approximately 3000; i.e., the counting rate increased from a background level of 12.5 to over 35,000 counts/sec. Clearly the release was heavy, so heavy, in fact, that significant quantities of gaseous fission products were released from the primary tank to the reactor building. For example, in an area with a normal background level of 2.3 mR/hr, surveys taken shortly after the release indicated an increase in radiation level to 250 mR/hr. Two types of activities were noted: one clearly airborne, presumably associated with krypton and xenon fission products; and the other which appeared on air filters and as a surface contamination. The results of gamma pulse-height analyses identified the latter as rare-gas daughters, almost entirely the 32-min ^{138}Cs. By 1620 on May 24, activity levels in the reactor building began to decrease. By 1115 on the following day, activity levels had decayed to normal.

Before, during, and after the release, no evidence of a FERD signal was noted. Cover-gas samples were taken shortly after the FGM annunciation. The results of analyses conducted on these indicated that a release had indeed occurred and that the S/N ratios for ^{133}Xe and ^{135}Xe were 100 and 400, respectively.

Samples of primary coolant were taken on May 24, 1967. Analyses were conducted for ^{137}Cs. The results indicated an activity level of 0.015 $\mu Ci/g$ of sodium. A comparison of these results with those derived from the three previous samples appeared at first to be confusing. The activity level in a sample taken on April 24, 1967, was measured as <0.005 $\mu Ci/g$ of sodium. On May 18 and 19 (approximately one week before the gas release), the levels had increased to 0.011 and 0.015 $\mu Ci/g$ of sodium respectively. Such results strongly implied the gradual loss of bond sodium during the period April 24 to May 18, 1967, followed on May 24 by a relatively massive gas release.

Attempts to identify the suspect were strongly influenced by the fact that the S/N ratio of the release was exceedingly high. From previous measurements of the S/N ratio for a single driver-fuel element,[4] it seemed clear that the release could not logically be attributed to driver fuel. To cause a signal of the strength measured, the fission-product inventories of approximately 300 driver-fuel elements would have been needed. Accordingly, a release from an encapsulated mixed-oxide fuel element was considered more logical. (At the time of the release, all experimental fuel elements were encapsulated.)

Using maximum fuel burnup as a criterion, three experimental subassemblies were removed from the core. The reactor was then operated for five days at 30 MWt without any evidence of an additional ARP. The inability to initiate an additional ARP was interpreted as evidence that the leaker was included in the group of subassemblies removed. Of these, X011 was reinstalled in the core. The reactor was restarted and, upon reaching a power level of 7.5 MWt, another release occurred. The reactor was shut down, X011 was removed, and the two remaining subassemblies in the original group of three were reinstalled. Operations proceeded without any evidence of additional releases until November 23, 1967 (see Sec. B below).

Subassembly X011 was transferred to the FEF and disassembled. Each capsule was inspected for visual evidence of damage. None was found. Neutron radiographs were then made of each of the 19 capsules. Of these, three (F4F, HOV4, and HOV10) were shown to contain deteriorated fuel elements. A series of six neutron radiographs showing the deterioration is given in Fig. 36. Of the six capsules shown, three--F4K, F4E, and F4F--were unchanged and were included merely to illustrate the quality of the radiographs.

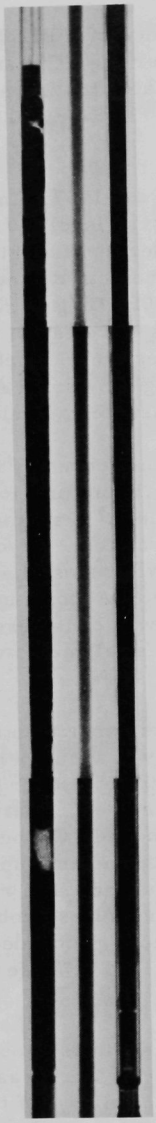

Neutron Radiographs of Damaged Capsules from Subassembly X011, ANL--HOV-4, GE--F4K

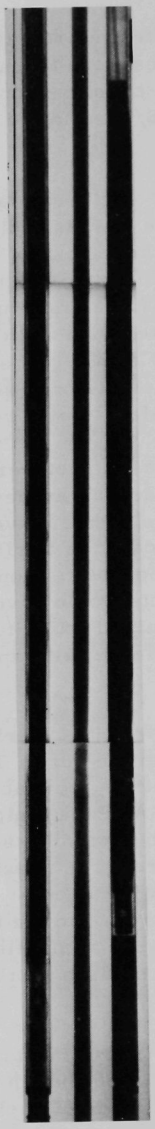

Neutron Radiographs of Damaged Capsules from Subassembly X011, GE--F4E, ANL--HOV-10

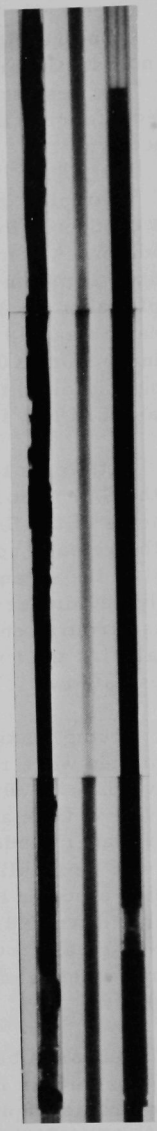

Neutron Radiographs of Damaged Capsules from Subassembly X011, GE--F4F, ANL--SOV-3

Fig 36. Neutron Radiographs of Encapsulated Experimental Fuel Elements from Subassembly X011. ANL Neg. No. 103-J5554.

Of the three capsules containing deteriorated fuel elements, one, HOV4, was eventually shown to be one that released fission products. The evidence included the following:

1. The element had suffered gross change.
2. The capsule released a small, but significant, amount of radioactive gas when placed in an evacuated chamber.
3. The capsule had lost weight by an amount equal to that of the original sodium bond.
4. The rare-gas fission-product inventory of the capsule was less than 1% of that expected from calculations based on fuel burnup.

B. ARP from X028: November 23, 1967 to May 6, 1968

The next series of ARP's began on November 23, 1967. In this series, several unusual phenomena were observed for the first time,[37-39] and since they illustrate many of the diagnostic concepts discussed earlier, the more important of them will be reviewed in detail.

The first release in the series occurred on November 23, 1967, during a normal ascent-to-power regime. Initial annunciation was again given by the FGM, which indicated a S/N ratio of approximately 18. The reactor was shut down, and cover-gas samples were taken and analyzed for ^{133}Xe and ^{135}Xe. Whereas a substantial increase was noted for ^{135}Xe (S/N ratio of 10), essentially none was noted for the longer-lived ^{133}Xe. The behavior of these species is shown in Fig. 37. The data provided an excellent example of an important diagnostic consideration. Until the time of the release, the ^{133}Xe activity remained relatively constant at approximately 2×10^{-4} μCi/ml. Almost all of this was tramp "holdover" from the previous run. A similar situation existed for ^{135}Xe; i.e., the activity before the startup of November 23 was of tramp origin. If the fuel element responsible for the release had been a "holdover" from the previous run, it, too, would have had its own holdover of ^{133}Xe activity. Hence, an increase should have been noted in the ^{133}Xe activity as a result of the release. The fact that no increase was noted was interpreted as almost certain proof that the suspect must have

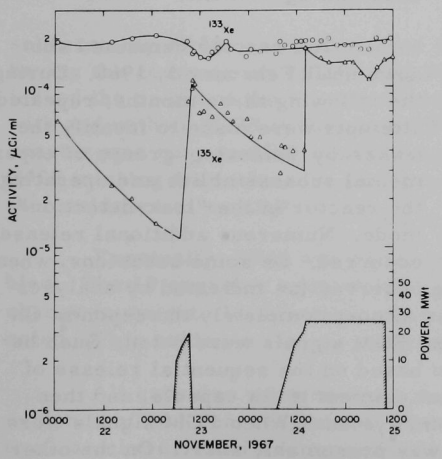

Fig. 37. Activities of ^{133}Xe and ^{135}Xe in Cover-gas Samples, November 22-25, 1967

been installed just before the startup. Fortunately, only six fresh fueled subassemblies had been added. These were C-2111 and C-2113 (both driver fuel), and four irradiation subassemblies.

The two driver-fuel subassemblies were removed, and the reactor was operated until December 6 without any significant evidence of an additional release. The inability to initiate an additional release during this period was interpreted as evidence that the leaker was one of the two driver-fuel subassemblies. (As discussed below, this conclusion was later proved erroneous.)

On December 6, 1967, the activity levels of both ^{133}Xe and ^{135}Xe began to increase and continued to increase until the end of run on December 10. The behavior of these species from November 28 to December 12 is shown in Fig. 38. Whereas all previous releases had been characterized by gas bursts, the release beginning on December 6 was clearly characteristic of one in which bond sodium, laden with ^{133}I and ^{135}I, was extruding at a continuous rate from either a driver element or an experimental capsule. A comparison of the buildup behavior of ^{135}Xe (Fig. 38) with the "fingerprint" data for a continuous bond leak (Fig. 7) demonstrates an excellent agreement.

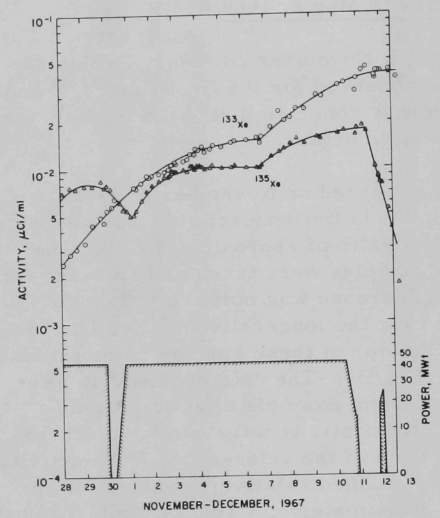

Fig. 38. Activities of ^{133}Xe and ^{135}Xe in Cover-gas Samples, November 28 to December 13, 1967

The reactor remained shut down until February 5, 1968. During the following three months, repeated attempts were made to identify the leaker by removing groups of experimental subassemblies and operating the reactor in the "leak-detection" mode. Numerous additional releases occurred. On some occasions, when large releases of ^{133}Xe and ^{135}Xe were observed (as indicated by analyses of cover-gas samples), the FGM failed almost completely to respond. On other occasions, large ^{133}Xe, ^{135}Xe, and FGM signals were noted. Such behavior indicated a release mechanism based on the sequential release of fission-product gas, first from the fuel element to its capsule, and then from the capsule to the primary sodium system. When FGM signals were seen, the delay between the releases was presumably short. On the other hand, when the delay was long, the FGM index species decayed in the capsule before the secondary release.

Another important phenomenon emerged during this series of fission-product releases. On several occasions, when the reactor was shut down and the primary pumps were turned off, secondary releases were observed. An example of this behavior is given in Fig. 39. Note that after pump shutdown, the levels of both ^{133}Xe and ^{135}Xe began to increase, passed through maxima, and then began to decay again. In both cases, the releases were characteristic of bond loss; i.e., the increases in ^{133}Xe and ^{135}Xe were gradual and continuous as their iodine parents decayed. If the ^{133}Xe and ^{135}Xe had originated in a gas release, the increases would have been sharp and discontinuous.

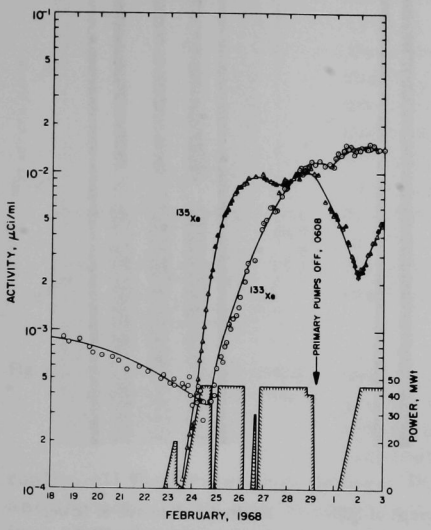

Fig. 39. Activities of ^{133}Xe and ^{135}Xe in Cover-gas Samples, February 18 to March 3, 1968

On other occasions, a consecutive reactor and pump shutdown led to the additional discharge of gaseous fission-product species. The mechanism common to both types of releases, i.e., sodium bond and gas, was presumably the relief of pressure in the capsule as a consequence of the pump shutdown.

Eventually, through a trial-and-error approach, the origin of the release was traced to experimental subassembly X028, which contained 19 encapsulated ternary metallic alloys having the composition 75% U, 15% Pu, and 10% Zr. Proof that X028 was indeed the origin of the many releases was provided by running the reactor with and without X028 in the core. Whenever X028 was in the core and the reactor was run, an ARP would occur shortly thereafter. Conversely, with X028 missing from the core the reactor would run indefinitely without further evidence of an ARP.

Eventually, X028 was removed from the reactor tank and disassembled. The 19 capsules were weighed. Of the 19, only one, BC02, showed a change in weight. In this case, a weight gain of approximately 11 g was noted. This evidence clearly marked BC02 as the prime suspect.

All capsules were neutron-radiographed. Only one, BC02, revealed evidence of fuel rearrangement. Radiographs of the upper third, midsection, and lower third are reproduced as Figs. 40-42. The radiographs

indicate that substantial quantities of fuel at the upper and lower ends of the pin melted and either flowed or slumped outward until confined by the colder capsule wall.

Fig. 40

Neutron Radiograph of Upper Section of Capsule BC02

Fig. 41

Neutron Radiograph of Mid-section of Capsule BC02

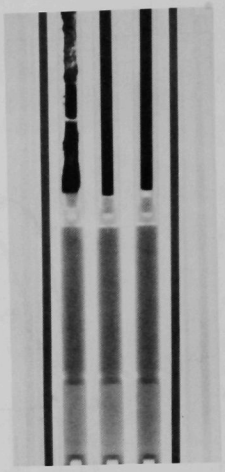

Fig. 42

Neutron Radiograph of Lower Section of Capsule BC02

A physical model of the capsule failure has been described in detail by Smith et al.[39] Basically, the model assumes flaws in both the fuel element and its surrounding capsule. Both flaws somehow escaped detection in the inspection program. Once the capsule was inserted in the reactor, pressure regimes were affected by reactor and primary-pump operation. The existence of two flaws, one in the element and one in the capsule, permitted a complex exchange of bond and primary-coolant sodium, and, on occasion, a release of stored-up fission-product gases. As Smith et al. have shown, the model satisfactorily explains most, if not all, of the experimentally observed phenomena.[38,39]

C. ARP from a Driver-fuel Element: Defect above Fuel Elevation

After the removal of X028 on May 6, 1968, reactor operations continued without incident for approximately four months. During a routine startup on September 7, 1968, however, the ^{135}Xe activity in the cover-gas samples was found to be significantly higher (by a factor of approximately two) than was measured for the previous run.[12] Such an increase suggested either an increase in the unavoidable tramp background component or an actual release of fission products from a defective fuel element. Since no increase was noted in the amplitudes of the FERD and FGM signals (both sensitive to the tramp background), the increase was regarded as real. A

reconstitution of the ^{135}Xe activity before and after the release is given in Fig. 43. Note that, whereas the equilibrium ^{135}Xe activity was approximately 4×10^{-3} μCi/ml during run 30A, it increased to over 7×10^{-3} μCi/ml near the end of run 30B. At no time during runs 30A or 30B was an increase noted in the FERD or FGM signals. Because of the gradual and continuous nature of the buildup curve for run 30B, a gas-type release was eliminated as a possibility. Rather, the mechanism appeared to be one in which sodium bond was being intermittently exchanged with the primary coolant. The strength of the signal, a S/N ratio less than two, tended to indicate that driver fuel was involved, since in all previous fission-product releases with encapsulated elements much larger signals were seen.[36,39]

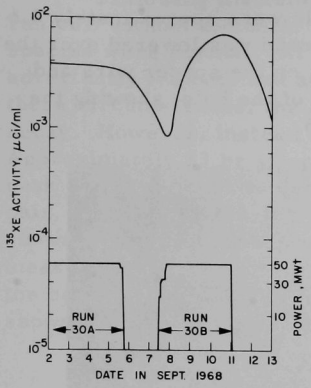

Fig. 43. Xenon-135 Activity during Runs 30A and 30B. ANL Neg. No. 103-L5170 Rev. 1.

Again, a trial-and-error method was used to locate the defective element. Large groups of driver-fuel subassemblies were removed and replaced, with either fresh fuel or fuel that had been previously exonerated. Eventually, all the driver fuel present during the run-30B startup was exonerated, and the conclusion was reached that the leaker was a driver element located in a control rod.

Advantage was taken of the fact that a control rod at its lowermost position generates 52% of the power that would be generated if the rod were fully inserted. Each rod, one at a time, was tested. The ^{135}Xe equilibrium activity was measured with a given rod fully inserted and with the same rod fully withdrawn. Eventually, a signal decrease was noted when control rod No. 2 was withdrawn. When the rod was again inserted, the signal increased. A reconstruction of the ^{135}Xe activity during the tests with control rod No. 2 is given in Fig. 44. Such behavior was regarded as proof that the control rod contained the defective element.

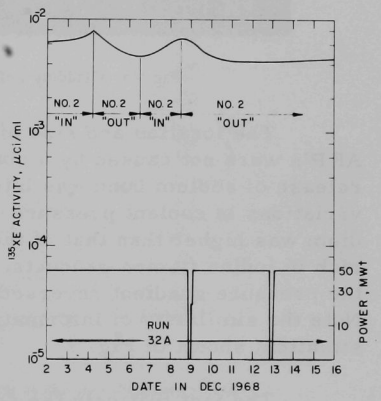

Fig. 44. Xenon-135 Correlation with the Position of Control Rod No. 2. ANL Neg. No. 103-L5174 Rev. 1.

Control-rod subassembly L-462 in the No. 2 control-rod position was removed. On the following startup, for run 32B, the ^{133}Xe and ^{135}Xe activities returned to the levels measured before the run-30B release.

During the postirradiation examination of the elements from L-462, one element was found to have an abnormally high sodium level. Upon closer visual inspection, a triangular hole under the upper spacer-wire weld was found in the cladding. The dimensions of the hole were approximately 1.6 x 7 x 24 mils. Apparently, when the hexagonal shroud was lowered over the assembled fuel bundle, the hexagonal can caught on the spacer wire and ripped the underlying weld loose. A photograph of the hole, showing the upper end of the spacer wire, is given in Fig. 45.

Fig. 45. Cladding Defect in Pin E57 from Subassembly L-462

The location and size of the hole clearly indicated that the observed ARP's were not caused by a continuous loss of sodium bond. Rather, the release of sodium bond was intermittent and was caused by short-term variations in coolant pressure. Whenever the internal pressure of the sodium was higher than that of the coolant, a small parcel of sodium bond, rich in iodine fission products, would leave the element. Conversely, when the pressure gradient reversed, primary sodium flowed into the element. Note the similarity of information given in Fig. 43 to that given for a Case-5 situation, shown in Fig. 7.

The fact that only the daughters of the long-lived halogens were observed is easily explained. The FGM index species, viz., ^{88}Kr, ^{89}Kr, and ^{138}Xe, have parents with exceedingly short half-lives, i.e., seconds. Hence, neither ^{88}Br, ^{89}Br, nor ^{138}I could live long enough to negotiate the path from their place of recoil birth, up through the bond, through the sodium reservoir above the fuel, and out through the defect. As they decayed en route, their daughters simply diffused upward into the fuel-element plenum.

D. ARP from a Driver-fuel Element: Defect below Fuel Elevation

Following the removal of L-462, the reactor was operated throughout run 32B without incident. During this time, the activity levels of all index species were normal. At 0903 on December 24, 1968, the reactor was inadvertently tripped, and at 1110 the primary pumps were turned off. Under these circumstances, the expected behavior of ^{135}Xe is a normal radioactive decay. However, instead of decaying, the ^{135}Xe activity began to increase.[13] Approximately 23 hr after pump shutdown, the activity passed through a peak and then began to decay in accordance with the half-lives of the $^{135}I/^{135}Xe$ pair. The ^{135}Xe behavior before, during, and after the pump shutdown is shown in Fig. 46. Subtraction of the calculated tramp activity from the measured total gives the ^{135}Xe activity associated with the release. Clearly, the release has essentially the same characteristics as the Case-7 situation shown in Fig. 9.

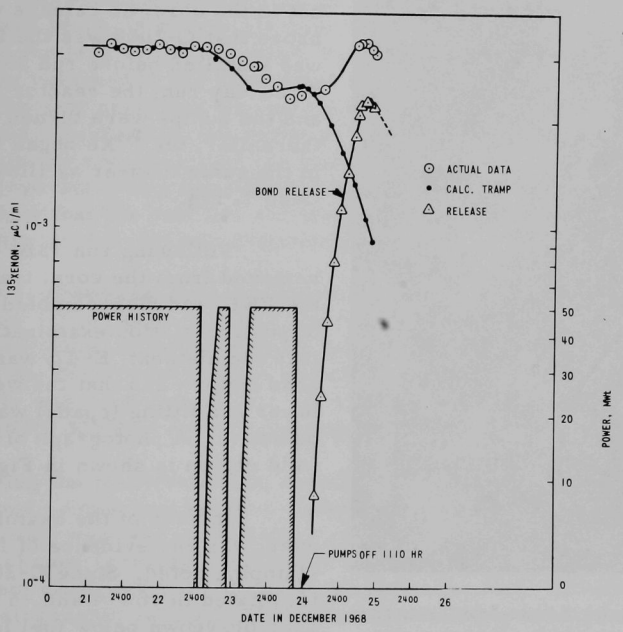

Fig. 46. Xenon-135 Activity in Cover Gas at End of Run 32B, Showing ^{135}Xe Buildup after Pump Shutdown. ANL Neg. No. 103-M5369.

In the manner discussed above in Sec. IV and V, the mechanism associated with the release involved a cladding defect in the region of the lower weld. During operation, the pressure component from the primary pumps tends to keep the sodium bond intact. In fact, under some circumstances, the pump pressure may actually force sodium into the element. Upon pump

shutdown, the reduction in coolant pressure permits bond sodium to extrude through the defect. By the time the pumps are shut down, all the shorter-lived halogen species in the bond have decayed. Iodine-133 and ^{135}I, however, live long enough to extrude and to give rise to their respective daughters.

The search for the leaker proved simple in this case. By a process of elimination, discussed by Fryer et al.[13] in detail, the search narrowed to a "half-worth" driver subassembly, C-2008, one used on numerous occasions for fine reactivity control in loading changes. In brief, Fryer reexamined the fission-product records and showed that whenever C-2008 was in the core, post-pump-shutdown releases occured (although the releases were often confused with others from X028 and L-462).

Fig. 47. Photograph of Lower-weld Region of the Defective Fuel Element from C-2008. ANL Neg. No. 103-L5100.

During run 33A, when C-2008 was not in the core, no release was noted. To prove that C-2008 was the leaker, C-2008 was installed before run 33B. After a three-day run, the reactor was shut down and the pumps were turned off. Shortly thereafter, the ^{135}Xe began to increase in the same manner as illustrated for Case 7, Fig. 9.

Following run 33B, C-2008 was removed from the core, transferred to the FEF, and disassembled. The results of postirradiation examination disclosed that one element, E-47, was deficient in bond sodium and that the weld at the lower end fitting (spade) was very likely defective. A photograph of the suspicious weld region is shown in Fig. 47.

In none of the examinations, however, was any evidence of fuel melting or slumping noted. Since C-2008 had been irradiated in row-4 and -5 locations, bond blowdown below fuel level was possible in principle. The fact that no unusual shortening or slumping was noticed suggests that bond-blowdown effects, if any, were probably characterized by channeling; i.e., the blowdown left enough sodium in the annulus to keep the fuel in the solid condition. In one sense, then, the results for C-2008 tend to verify the results of the partially bonded TREAT tests (EBR-MF-1 and -2) and the results of heat-transfer calculations.

IX. DEFECT SIMULATION STUDIES IN EBR-II

To provide more information relating to the annunciation and consequences of inadvertent driver-fuel cladding failures, two in situ studies were conducted in EBR-II.[40] In the first of these, a standard driver element with a known defect in the upper weld region was used. In the second, a contrived defect was formed at the spade end of an otherwise standard driver-fuel element. Both specimens were irradiated in EBR-II, and the effects of the respective defects were observed. Following the irradiations, the test specimens were examined both nondestructively and destructively. Since the details of these tests have been presented elsewhere,[40] only the more important results will be cited here.

A. Upper-leaker Experiment

The fuel element selected as the test specimen consisted of an otherwise standard Mark-IA driver element with a leak in the region of the upper weld. Once the leak was discovered, during postfabrication inspection, the element was returned to the production line and impact-bonded in the normal manner. The test specimen was weighed, gauged, X-rayed, and neutron-radiographed. Aside from the known defect, the specimen was in all respects within the specifications for standard driver-fuel elements. Just before incorporation into the subassembly, the specimen was again leak-tested to show that the hole had not been plugged. From leak-rate data a hole diameter of 0.5 mil was estimated.

The test vehicle, Subassembly C-2194S, was installed in the core in grid position 3C1 on May 14, 1969. Despite intensified efforts at fission-product monitoring, no release was ever noted. Accordingly, it was concluded that the defect had plugged sometime after the final leak test. The subassembly was removed on July 16, 1970, at a maximum fuel burnup of 0.63 at. % (5700 MWd of reactor operation).

During the postirradiation examinations, the test specimen was weighed, bond-tested, and neutron-radiographed. In addition, the top weld of the specimen was leak-tested after sectioning. The results indicated no significant change in weight (within the accuracy limits of the balance) and no significant change in the sodium level above the fuel. Similarly, the neutron-radiographic results failed to reveal anything unusual.

Because all evidence indicates that the defect in the upper weld region became plugged before a fission-product release could occur, the results of the tests must be regarded as inconclusive.

B. Lower-leaker Experiment

The test specimen used in this experiment consisted of an otherwise standard driver-fuel element with a 3-mil hole in the lower end fitting

(spade). The test specimen and two controls (normal fuel elements) were weighed, measured, X-rayed, and neutron-radiographed before their incorporation in a standard driver-fuel subassembly (C-2250S). To avoid excessive oxidation of sodium in the vicinity of the leak, a small temporary closure weld had been made at the bottom of the spade, and this was drilled free immediately before the test specimen was assembled in the test vehicle. Within 1 hr, the test vehicle was inserted in a temporary argon-filled coffin. Approximately 30 min later, the test vehicle was transferred to the fuel unloading machine and in another 90 min was placed in the reactor storage basket.

The first power operation began on January 14, 1970. Between this date and January 28, three reactor and pump shutdowns occurred. In all cases a small but significant increase was noted in the ^{135}Xe activity after the pump shutdown.

Qualitatively, the behavior of the ^{135}Xe activity after a pump shutdown agreed well with those observed for the C-2008 releases.[13] On the other hand, a major difference was noted during steady-state operation. In the case of C-2008, the only signal increase occurred after pump shutdown. During steady-state operation no signal was noticed. Before C-2250S was installed in the core, the equilibrium ^{135}Xe background was 3.0×10^{-3} $\mu Ci/ml$. After C-2250S was installed, the background (with the reactor running) increased to an equilibrium value of 8×10^{-3} $\mu Ci/ml$. Proof that this effect was real was indicated by the return to normal background levels when C-2250S was removed temporarily. A subsequent reinsertion of C-2250S in the core caused the steady-state background to increase to approximately 8×10^{-3} $\mu Ci/ml$. When a reactor and pump shutdown on March 27 failed to cause an additional release, the test vehicle was removed from the core in preparation for postirradiation examination.

Although the steady-state signal from C-2250S has never been explained unambiguously, it seems likely that the mechanism involved was the intermittent loss of sodium bond through the defect. Such behavior was, of course, noticed during the residence of L-462 in the core.[12] Apparently, the size of the defect is a critical factor in determining whether intermittent bond-loss phenomena are important. Thus, the hole sizes for L-462 and C-2250S were large enough, whereas the hole size for C-2008 was too small.

The test element from C-2250S, the two control elements from this subassembly, and the defective element from C-2008 were subjected to detailed postirradiation examinations. As a result of these examinations it was shown that (1) the test element from C-2250S lost approximately 0.5 g during its irradiation, (2) the sodium level in the test element was abnormally low, (3) the external appearance of the test element was normal in all respects, (4) no length change was noted for the fuel in the test element,

(5) a small bulge in the cladding was noted near the bottom of the test element, (6) the fuel material in the test element had not swelled against the cladding, and (7) the microstructure of the fuel material in the test element indicated that the fuel material had not lost its heat-transfer capability.

Perhaps the most significant achievement resulting from this test was the additional verification that fuel elements known to be subject to bond losses can, in fact, be operated in the EBR-II core without any evidence of hazard.

X. CONSEQUENCES OF OPERATING WITH DEFECTIVE DRIVER-FUEL ELEMENTS

Sustained operation of the reactor with one or more defective driver-fuel elements will increase the concentrations of rare-gas fission products in the cover-gas plenum and "solid" fission products in the primary coolant system. If the number of defective elements should become excessively large, it is conceivable that (1) the ability of the fission-product monitoring systems to annunciate additional releases would be compromised, (2) the normal leakage of cover gas to the reactor building would cause radiological problems, and (3) the accumulation of entrained fuel material in the primary sodium would cause a troublesome increase in the normal tramp background. These possibilities are reviewed below in an effort to define the maximum number of defective driver-fuel elements that can be tolerated under sustained operation conditions.

A. Effects of Sustained Defective-fuel Operation on the Ability to Annunciate Failures

Of principal interest is the number of defective driver-fuel elements that can be tolerated without compromising the ability to annunciate an additional failure.

In the discussion that follows, the tacit assumption is made that any fission-product release causing a 10% increase in signal is detectable. Also assumed is the credible, but unlikely, release of the entire fission-product inventory of a driver-fuel element located in row 1. As a final, very conservative assumption, it is assumed that a number of fuel elements located in row 1 fail simultaneously. The problem, then, is to determine the maximum number of such elements that can be tolerated without compromising the ability to detect the complete release of fission products from another row-1 element. An ideal starting point for an evaluation of this nature is the S/N ratio measured for a single completely unclad fuel pin. As Smith *et al.*[5] have shown, the S/N ratio for an unclad fuel pin located in a row-1 position would be approximately 5. If n is the number of completely unclad fuel pins in a row-1 position and if a S/N ratio of 0.10 is detectable, then the background from n - 1 pins will be 5(n - 1) + 1, whereas the signal from the nth pin will be simply 5. Hence,

$$S/N = 0.10 = \frac{5}{5(n-1)+1}. \qquad (50)$$

The solution for Eq. 50 is $n \simeq 11$. That is, 10 completely unclad fuel elements can be tolerated before background effects from these 10 cause the S/N ratio for the 11th to decrease to 0.1.

Although the above treatment relies on rather simplifying assumptions, the estimate of 10 is regarded as realistic. Admittedly, the assumptions

of a 100% fission-product release are unrealistic, but in the treatment described above, such an assumption is not seriously compromising. In practice, the S/N ratio for an actual release may average 2. However, if the nth failure also gave a S/N of 2, the number of tolerable previous failures would still be approximately 10.

B. Radiological Effects of Fission-product Leakage to the Reactor Building

Although definitive information relating to the leakage of fission products to the reactor building is seriously lacking, some first-order (conservative) estimates can nevertheless be made. Two items of information can be used as a basis for such estimates: (1) the results of radiological surveys conducted during exposed-fuel calibration studies,[5] and (2) the results of radiological surveys conducted after inadvertent ARP's from experimental fuel elements.

As a preface to the discussion that follows, rare-gas fission products can leak to the reactor building from the primary cover-gas system through a variety of static and dynamic seals. As discussed elsewhere,[5] static seals consist essentially of solid, soft copper gaskets in the form of O-rings compressed between steel flanges. Leakage through such seals is considered unlikely. Leakage around dynamic seals, on the other hand, is not only possible but likely. Of 29 dynamic seals around penetrations through the primary-tank cover and rotating shield plugs, 20 are stainless steel bellows. The latter are regarded as leaktight. The remaining nine are associated with the holddown column, the core gripper, the two cover-lift columns on the small rotating plug, the storage-basket column, the transfer arm, the transfer port, and the two primary pumps in the primary-tank cover. Leakage from and around these seals accounts for essentially all the radioactivity that enters the reactor building after an ARP.

1. Results of Exposed-fuel Calibration Studies

In these tests, two completely unclad Mark-IA driver-fuel pins were irradiated under 50-MW operating conditions for approximately 5.5 days. During this time, all the index species for the various monitoring systems, with the exception of ^{133}Xe, either achieved or closely achieved their respective equilibrium values. Throughout the tests, attempts were made to detect and to measure, if possible, the leakage of rare-gas fission products to the reactor building. As discussed in detail elsewhere,[5] no perceptible increase was noted in the general radiological background in the reactor building. Although such results were clearly negative, the inference is clear; at least two defective driver-fuel elements can be tolerated without measurably affecting radiological conditions in the reactor building.

2. Results of Inadvertent ARP's from Experimental Fuel Elements

Clearly, the inability to detect fission-product leakage to the reactor building during the exposed-fuel tests was the result of an inadequate signal. Larger signals have been generated, however, on numerous other occasions from either X001 or X028. Information derived from these releases can be used to establish an approximate range for the number of defective driver-fuel elements that can be tolerated before activity is leaked to the reactor building.

Thus far, three ARP's have been large enough to have been sensed by monitoring equipment in the reactor building. The first, and incidentally the largest release experienced in EBR-II, occurred on May 24, 1967. At this time, the ^{133}Xe and ^{135}Xe activities in the cover gas peaked at 2.3 and 1.8 $\mu Ci/ml$, respectively. As discussed in detail elsewhere,[36] detectable amounts of radioactivity were leaked to the reactor building.

The second release that led to off-normal activity levels in the reactor building originated from Subassembly X028 on April 6, 1968.[39] Activity levels measured for ^{133}Xe and ^{135}Xe in the cover gas were 0.28 and 0.22 $\mu Ci/ml$, respectively. The release of radioactive gases to the reactor building was, in this case, considerably smaller than for the release of May 24, 1967. Radiation levels on air-particulate monitoring systems increased by a factor of approximately 50%, whereas in the release of May 24, 1967, increases of the order of 100 were noted. The difference between these two situations was due to the much larger release of short-lived gaseous species during the May 24 release.

The third release, also originating from X028, occurred on April 19, 1968. In this case, the signal from an air-particulate monitoring system increased by a factor of about 10. The results of cover-gas analyses indicated levels of 0.35 and 0.2 $\mu Ci/ml$ for ^{133}Xe and ^{135}Xe, respectively.

Although the limits of permissible driver-fuel failures cannot be specified, useful guidelines can be generated from the release data of April 6, 1968. In this case, concentrations of 0.28 and 0.22 $\mu Ci/ml$ were sufficient to permit detection in the reactor building. If detectability is used as a criterion of unacceptability, then a value of approximately 0.25 $\mu Ci/ml$ for either ^{133}Xe or ^{135}Xe in the cover-gas system can be used as a guideline. The results of the exposed-fuel studies can be used to show that a single unclad fuel pin located in a row-1 position can, under 62.5-MWt operating conditions, lead to an equilibrium level of 0.010 $\mu Ci/ml$ for either ^{133}Xe or ^{135}Xe. Hence, if 0.25 $\mu Ci/ml$ is the activity level above which leakage to the reactor building can be detected, as many as 0.25/0.010 or 25 completely unclad fuel elements can be tolerated. In practice, a larger number is implied. The estimate above is based on a S/N ratio of 5, which

is essentially an upper limit for a driver fuel element. Since S/N ratios of 5 seem unlikely for actual releases, the estimate of 25 should be regarded as conservative.

C. Effects of Entrained Fuel Material on Tramp Background

If the reactor is operated with substantial amounts of exposed fuel in the core, fuel material can conceivably erode from the surface and become either mechanically or chemically entrained in the primary coolant. In that event, the normal tramp fission-product component would increase and could, under extreme circumstances, be troublesome.

The amount of ^{235}U contamination needed to produce the normal tramp background has been estimated by coauthor E. R. Ebersole to be 2 mg. Although definitive measurements of the effective "dissolution" rate of fuel material under hot, flowing-sodium conditions have not been made, limited information derived during exposed-fuel studies[5] can be used as an upper limit. Before and after two completely unclad fuel pins were installed in the core, primary-sodium samples were taken and analyzed for uranium. Within the sensitivity of the method, no uranium was found. Since the sensitivity of detection was 0.2 ppb, it is simple to show that the upper limit to the dissolution rate of fuel material from the pin was less than 2.7 mg of fuel material per day per fuel pin (assuming, of course, that the uranium remains in the primary sodium).

The amount of exposed fuel that could, hypothetically, be tolerated in the core without seriously affecting the tramp background can be estimated under the following assumptions: (1) the primary-coolant inventory in the core is approximately 50 liters, (2) the total primary-coolant inventory is 2.4×10^6 liters, (3) the dissolution rate of fuel material from an unclad fuel pin is 2.7 mg/day (or 1.4 mg ^{235}U/day), (4) all fuel material removed remains suspended in the coolant, and (5) the average residence of a fuel element is approximately 80 days of full-power operation. Assuming the above conditions, as many as 1000 completely unclad fuel pins could reside in the core for their entire useful lives before background effects from fuel dissolution equaled those from tramp uranium.

Clearly, the extent of fuel exposure during any given driver-fuel-element failure would be far less than total. Accordingly, the estimates given above must be considered extremely conservative. From such considerations, the conclusion follows that the dissolution of fuel material from a defective driver-fuel element is of no significance.

XI. SUMMARY AND CONCLUSIONS

1. The five fission-product monitoring systems used at EBR-II (three on-line and two off-line) supply overlapping information that can be used to differentiate between gas-type and bond-type releases and to distinguish between releases from driver-fuel elements and experimental fuel elements.

2. The time behavior of tramp-origin ^{133}Xe and ^{135}Xe in the cover gas can be accurately predicted from the time-power history of the reactor.

3. The pressure in the gas plenum of a driver element depends on its location in the reactor, the fuel burnup, the fuel type, and the initial bond level.

4. Depending primarily on location in the reactor, a cladding defect below fuel elevation may lead to substantial unbonding of driver fuel. Under a combination of adverse conditions, fuel material in row 6 may unbond as much as 8.0 in.; in row 5, 6.0 in.; and in row 4, 2.4 in. Unbonding cannot occur in rows 1-3 because of the dynamic coolant pressure against the defect.

5. Cladding defects above fuel elevation cannot lead to unbonding. Depending on the location, such defects may either release filling gas (and rare-gas fission products) or sodium bond. A combination of the two types of release is also possible.

6. Defects anywhere below the bond level may lead to the intermittent extrusion of sodium bond that is rich in iodine fission products. Such releases cannot easily be distinguished from the slow continuous extrusion of sodium bond.

7. All fission-product gas releases are characterized by sharp and discontinuous increases in cover-gas activity levels for the gaseous index species. All such releases are also characterized by an almost immediate decay in accordance with the half-lives of the respective index species.

8. All loss-of-bond-type releases are characterized by the release of halogen fission products to the primary coolant system. The time-dependent buildup of their respective rare-gas daughters can be used as an indication of the nature of the release. A sharp burst-type release of sodium bond leads to a prominent predictable peaking of the rare-gas activities. A slow continuous release of sodium bond, on the other hand, leads to a much broader peak with the time of peaking considerably delayed.

9. Relaxation of the dynamic coolant pressure against a defect by turning off the primary-coolant pumps (after a reactor shutdown) has proved to be a valuable diagnostic aid. On numerous occasions, a reactor and primary-pump shutdown has led to secondary ARP's, sometimes gas, sometimes sodium bond, and sometimes a combination of the two.

10. Considerable success has been achieved in explaining the time-dependent behavior of fission products for the various types of releases in mathematical terms.

11. The results of previous exposed-fuel calibration studies have proved extremely useful in placing fission-product release kinetics on a quantitative base.

12. The hypothetical case of an instantaneous loss of all bond under EBR-II operating conditions was simulated in TREAT. The results demonstrated that although fuel material melts, it flows to the colder cladding and immediately freezes, with the result that heat transfer is reinitiated.

13. The short-term effects of operating an EBR-II fuel element with large circumferential and essentially infinite longitudinal voids were also simulated in TREAT. The results indicated that even under equivalent EBR-II conditions of 90 MWt, voids as long as 9 in. in length and 180° in arc could be tolerated without noticeable fuel melting, slumping, or rearrangement. The results of first-principle heat-transfer calculations were consistent with these observations.

14. Eight verified series of ARP's have occurred in EBR-II. The first two were associated with encapsulated experimental fuel elements (X011 and X026), three originated from driver-fuel elements, and three others originated from unencapsulated mixed-oxide elements. In all cases, experimental information relating to fission-product behavior was understandable in terms of physical models and the respective half-lives of the various fission-product index species.

15. A fuel element having a known defect in the upper weld region was irradiated to a maximum burnup of 0.63 at. % without any evidence of an ARP. All available evidence suggested that the defect became plugged, very likely with sodium oxide.

16. A fuel element with a 3-mil contrived defect in the lower end fitting was also irradiated. In this case, relatively strong signals were seen during operation. Following reactor and primary-pump shutdowns, secondary releases were also evident.

17. As many as 10 defective driver-fuel elements can be tolerated indefinitely without compromising the ability to annunciate an additional failure.

18. As many as 25 defective driver-fuel elements can be tolerated indefinitely before fission-product leakage effects to the reactor building become detectable.

19. Fuel dissolution during defective-fuel operation has an inconsequential effect on the normal tramp background.

ACKNOWLEDGMENTS

The authors gratefully acknowledge the help and cooperation of Messrs. G. E. Deegan, J. R. Davis, F. S. Kirn, and other personnel of the EBR-II Operations group. Equal appreciation is expressed to Messrs. M. J. Feldman, N. R. Grant, D. C. Hampson, and D. L. Mitchell of the Fuels and Examination Facility.

REFERENCES

1. L. J. Koch, H. O. Monson, D. Okrent, M. Levenson, W. R. Simmons, J. R. Humphreys, J. Haugsnes, V. Z. Jankus, and W. B. Loewenstein, *Hazard Summary Report: Experimental Breeder Reactor II (EBR-II)*, ANL-5719 (May 1957).

2. L. J. Koch, W. B. Loewenstein, and H. O. Monson, *Addendum to Hazards Summary Report: Experimental Breeder Reactor-II (EBR-II)*, ANL-5719 (Addendum) (June 1962).

3. R. R. Smith and C. B. Doe, *Fission Product Monitoring in EBR-I, Mark IV*, ANL-6788 (Jan 1964).

4. R. R. Smith and C. B. Doe, *Cladding Failure Simulation Tests in EBR-II*, ANL-7067 (Dec 1966).

5. R. R. Smith, C. B. Doe, and E. R. Ebersole, *Exposed-fuel Calibration Study in EBR-II, Second Series*, ANL-7558 (Jan 1970).

6. K. G. Porges, "EBR-II Fuel Element Failure Detector," *Reactor Physics Division Annual Report: July 1, 1963 to June 30, 1964*, ANL-7010, p. 231 (Jan 1965).

7. K. G. Porges and A. De Volpi, "Design Improvements and Sensitivity Tests of the FERD System for EBR-II," *Reactor Physics Division Annual Report: July 1, 1964 to June 30, 1965*, ANL-7110, pp. 294-295 (Dec 1965).

8. G. S. Brunson, *On-line Noble Gas Fission Product Monitoring in EBR-II*, Nucl. Tech. *10*, 33-34 (Jan 1971).

9. R. R. Smith, W. B. Loewenstein, and C. M. Walter, *The EBR-II: A Status Report*, ANL-7743 (July 1971).

10. J. P. Bacca, F. G. Foote, G. C. McClellan, and J. H. Cook, *Performance of EBR-II Driver Fuel*, Trans. Am. Nucl. Soc. *12*(1), 90 (June 1969).

11. P. B. Henault, *On the Unbonding of the EBR-II Driver-fuel Element*, ANL-7819 (to be published).

12. R. M. Fryer, E. R. Ebersole, P. B. Henault, and R. R. Smith, *Symptoms and Detection of a Fission-product Release from an EBR-II Fuel Element: Case 1. Defect above Fuel Elevation*, ANL-7605 (Jan 1970).

13. R. M. Fryer, R. R. Smith, E. R. Ebersole, and R. V. Strain, *Symptoms and Detection of a Fission-product Release from an EBR-II Fuel Element: Case 2. Defect below Fuel Elevation*, ANL-7676 (June 1970).

14. G. A. Freund, P. Elias, D. R. MacFarlane, J. D. Geier, and J. F. Boland, *Design Summary Report on the Transient Reactor Test Facility (TREAT)*, ANL-6034 (June 1960).

15. F. S. Kirn, J. Bowland, H. Lawroski, and R. Cook, *Reactor Physics Measurements in TREAT*, ANL-6173 (Oct 1960).

16. C. E. Dickerman, R. D. Johnson, and J. Gasidlo, *Kinetics of TREAT Used as a Test Reactor*, ANL-6458 (May 1962).

17. A. De Volpi and C. H. Freese, *Fast Neutron Transient Detections Hodoscope for Reactor Fuel Meltdown Studies*, IEEE Trans. Nucl. Sci. *NS-13*(1), 623 (1965).

18. E. S. Sowa and J. C. Heap, *The Development of a Small Integral Sodium Loop for In-pile Fuel Failure Studies in the Presence of Flowing Sodium*, Trans. Am. Nucl. Soc. *8*(2), 559 (1965).

19. C. E. Dickerman *et al.*, *TREAT Sodium Loop Experiments on Performance of Unbonded, Unirradiated EBR-II Mark I Fuel Elements*, Nucl. Eng. and Design *12*, 381-390 (1970).

20. F. L. Willis, C. E. Dickerman, P. B. Henault, R. Purviance, J. F. Boland, and R. Noland, *TREAT Experimental Study of Survival of EBR-II Fuel Pin in a Loss-of-Bond Incident*, Trans. Am. Nucl. Soc. *11*(2) (1968).

21. C. E. Dickerman, R. R. Smith, F. L. Willis, A. B. Cohen, and R. Regis, *Analysis of Transient Behavior of Unbonded EBR-II Fuel Pin Incident*, Trans. Am. Nucl. Soc. *11*(2) (1968).

22. C. E. Dickerman, F. L. Willis, R. Smith, and A. B. Cohen, "Fast Reactor Safety Integral Loop Experiment on an Argon-Bonded EBR-II Pin," *Reactor Physics Division Annual Report: July 1, 1966 to June 30, 1967*, ANL-7310, pp. 258-260 (Jan 1968).

23. C. E. Dickerman, R. Purviance, L. E. Robinson, W. Stephany, and F. L. Willis, *Summary and Analysis of TREAT Sodium Loop Experiments on Behavior of Single EBR-II Mark I Pins under Accident Conditions*, Nucl. Eng. and Design *7*, 442 (1968).

24. D. F. Schoeberle, J. Heestand, and L. B. Miller, *A Method of Calculating Transient Temperatures in a Multiregion, Axisymmetric, Cylindrical Configuration. The ARGUS Program, 1089/RE248, Written in FORTRAN II*, ANL-6654 (Nov 1963).

25. C. M. Walter and L. R. Kelman, *Penetration Rate Studies of Stainless Steel by Molten Uranium and Uranium-Fissium Alloy*, J. Nucl. Mat. *6*, 281 (1962).

26. C. M. Walter and C. E. Dickerman, *TREAT Study of the Penetration of Molten Uranium and U-5 wt % Fs Alloy through Type 304 Stainless Steel*, Nucl. Sci. Eng. *18*, 518 (1964).

27. *Reactor Development Program Progress Report: August 1969*, ANL-7606, pp. 62-63 (Sept 26, 1969).

28. *Reactor Development Program Progress Report: September 1969*, ANL-7618, pp. 66-69 (Oct 27, 1969).

29. *Reactor Development Program Progress Report: November 1969*, ANL-7640, pp. 73-75 (Dec 31, 1969).

30. J. C. Hesson, M. J. Feldman, and L. Burris, *Description and Proposed Operation of the Fuel Cycle Facility for the Second Experimental Breeder Reactor (EBR-II)*, ANL-6605 (Apr 1963).

31. S. T. Zegler and M. V. Nevitt, *Structures and Properties of Uranium-Fissium Alloys*, ANL-6116 (July 1961).

32. G. L. Stephens and D. J. Campbell, *Program THTB for Analyses of General Transient Heat Transfer Systems*, G. E. Report R60FPD647 (Apr 1961).

33. R. R. Smith, R. A. Cushman, R. W. Hyndman, F. S. Kirn, J. K. Long, W. B. Loewenstein, J. T. Madell, T. R. Bump, and P. J. Persiani, "Recent Operating Experience with EBR-II," *Proceedings of the BNES Conference on the Physics of Fast Reactor Operation and Design*, London, England (June 1969).

34. R. R. Smith, C. B. Doe, and F. S. Kirn, *The Application of Cover-gas Monitoring in the Recent EBR-II Fission-product Release*, Trans. Am. Nucl. Soc. *10*(2),634 (Nov 1967).

35. E. R. Ebersole and R. Villarreal, *Diagnostic Radiochemistry Following the Recent EBR-II Fission-product Release*, Trans. Am. Nucl. Soc. *10*(2), 634 (Nov 1967).

36. R. R. Smith, D. W. Cissel, C. B. Doe, E. R. Ebersole, and F. S. Kirn, *Locating and Identifying the Source of the May 24, 1967 Fission-product Release in EBR-II*, ANL-7543 (Apr 1969).

37. R. R. Smith, E. R. Ebersole, and F. W. Thalgott, *Experience with a Gas-type Failure in an EBR-II Driver Fuel Element*, Trans. Am. Nucl. Soc. *11*(1), 279 (June 1968).

38. R. R. Smith, E. R. Ebersole, R. M. Fryer, and P. B. Henault, *Fission-product Release from an Encapsulated U-Pu-Zr Alloy*, Trans. Am. Nucl. Soc. *12*(1), 180 (June 1969).

39. R. R. Smith, E. R. Ebersole, R. M. Fryer, and P. B. Henault, *Origin of Fission-product Releases in EBR-II, November 23, 1967, to May 6, 1968*, ANL-7604 (Dec 1970).

40. G. S. Brunson, R. M. Fryer, and R. V. Strain, *Experimental Irradiations of Fuel Elements Having Known Cladding Defects in EBR-II*, ANL-7782 (July 1971).